NASA TECHNICAL NOTE

NASA TN D-8445

AN INVESTIGATION OF THE TEMPORAL CHARACTER OF MESOSCALE PERTURBATIONS IN THE TROPOSPHERE AND STRATOSPHERE

William W. Vaughan

George C. Marshall Space Flight Center
Marshall Space Flight Center, Ala. 35812

NATIONAL AERONAUTICS AND SPACE ADMINISTRATION • WASHINGTON, D. C. • MARCH 1977

1. REPORT NO. NASA TN D-8445	2. GOVERNMENT ACCESSION NO.	3. RECIPIENT'S CATALOG NO.
4 TITLE AND SUBTITLE An Investigation of the Temporal Character of Mesoscale Perturbations in the Troposphere and Stratosphere		5. REPORT DATE March 1977
		6. PERFORMING ORGANIZATION CODE
7. AUTHOR(S) William W. Vaughan		8. PERFORMING ORGANIZATION REPORT # M-217
9. PERFORMING ORGANIZATION NAME AND ADDRESS George C. Marshall Space Flight Center Marshall Space Flight Center, Alabama 35812		10. WORK UNIT NO.
		11. CONTRACT OR GRANT NO.
		13. TYPE OF REPORT & PERIOD COVERED
12. SPONSORING AGENCY NAME AND ADDRESS National Aeronautics and Space Administration Washington, D.C. 20546		Technical Note
		14. SPONSORING AGENCY CODE

15. SUPPLEMENTARY NOTES

Prepared by Space Sciences Laboratory, Science and Engineering

16. ABSTRACT

The purpose of this investigation was to assess the effectiveness of mesoscale models in explaining perturbations observed in vertical detailed wind profile measurements in the troposphere and lower stratosphere. The structure and persistence of the data were analyzed and interpreted in terms of several physical models with the goal of establishing explanations for the observed persistent features of the mesoscale flow patterns.

The experimental data used in the investigation were obtained by a unique detailed wind profile measurement system. This system is capable of providing resolution of 50 to 100 m wavelengths for the altitude region from approximately 200 m to 18 km. The system consists of a high-resolution tracking radar and special super-pressure balloon configuration known as a Jimsphere.

17. KEY WORDS Gusts Mesoscale Troposphere Wind Profiles	18. DISTRIBUTION STATEMENT 47

19. SECURITY CLASSIF. (of this report) Unclassified	20. SECURITY CLASSIF. (of this page) Unclassified	21. NO. OF PAGES 87	22. PRICE $5.00

* For sale by the National Technical Information Service, Springfield, Virginia 22161

ACKNOWLEDGMENTS

TABLE OF CONTENTS

LIST OF ILLUSTRATIONS

LIST OF ILLUSTRATIONS (Continued)

LIST OF ILLUSTRATIONS (Continued)

LIST OF ILLUSTRATIONS (Concluded)

AN INVESTIGATION OF THE TEMPORAL CHARACTER
OF MESOSCALE PERTURBATIONS IN THE
TROPOSPHERE AND STRATOSPHERE

I. INTRODUCTION

This research is concerned with the analysis of mesoscale perturbations as revealed by detailed wind profile measurements in the troposphere and lower stratosphere. If measurements of the detailed wind profile structure above the planetary boundary layer (approximately the first kilometer of atmosphere) are examined carefully, fluctuations with a wide range of length and time scales may be observed. One way of viewing the nature and characteristics of these fluctuations is by considering perturbations about a mean wind profile which should remain constant — or nearly constant — throughout a period of several hours. These perturbations, which vary in wavelength and amplitude, may be broadly categorized as macroscale (frequently referred to as synoptic scale), mesoscale, and microscale. The macroscale perturbations have a vertical wavelength generally greater than 10 km and velocity amplitudes greater than 20 m s^{-1}. These perturbations are usually persistent with time and are attributed to the macroscale and large pressure and temperature structure of the atmosphere. The microscale perturbations have a vertical wavelength of less than approximately 1500 m and an amplitude of approximately 6 m s^{-1}. Microscale perturbations form the turbulent part of the wind profile and are highly transient in nature. Turbulence is used in a rather loose context and does not necessarily possess all the characteristics of true turbulence, i. e., vorticity, three-dimensionality, etc.

Mesoscale horizontal wind perturbations have vertical wavelengths of approximately 1 to 3 km and amplitudes of approximately 15 m s^{-1}. Individual mesoscale perturbations persist for varying periods of time and appear to be associated with a variety of generating mechanisms. The division of the vertical wind profile structure into macroscale, mesoscale, and microscale categories is arbitrary and may not reflect a natural physical preference or division of the wind structure into discrete categories of wind perturbations, at least not insofar as can be ascertained from a spectral investigation (see Section III) of the vertical wind profile structure. Accordingly, the designation "mesoscale" as used in this study is understood as being generally within the range of the definition previously given.

Before proceeding into the analysis of the mesoscale perturbations as revealed by the series of detailed wind profile measurements obtained at approximately 2 h intervals during a period of 10 to 12 h, a review of the literature is given. The literature contains many references to mesoscale flow in the atmosphere, above the boundary layer, as characterized by the wave structure noted in the wind perturbations observed in tropospheric and stratospheric detailed wind profile measurements. Observations of systematic features of such waves and the challenge for explanation predates the development of modern detailed wind flow measurement systems. In 1889, Helmholz, as noted by Goldie (1925), declared:

> It appears to me not doubtful that such systems of waves
> occur with remarkable frequency at the boundary surface of
> strata of air of different densities, even although in most cases
> they remain invisible to us. Evidently, we see them only when
> the lower stratum is so nearly saturated with aqueous vapor that
> the summit of the wave, within which the pressure is less, begins
> to form a haze. Then, there appear streaky parallel trains of
> clouds of very different breadths, occasionally stretching over the
> broad surface of the sky in regular patterns. Moreover, it seems
> to me probable that this which we thus observe under special con-
> ditions that have rather the character of exceptional cases, is
> present in innumerable other cases when we do not see it.

Goldie (1925) also studied the subject and endeavored to relate surface variations in pressure and winds with the upper air data available at the time. The lack of adequate upper air data significantly hindered his studies. Taylor (1917) in his classic paper on the nature of turbulent motion noted that gusts not due to action of pressure variations must have derived their high velocity from some other faster-moving layer of the air. The ageostrophic flow as reflected in the mesoscale perturbations and the probable influence by wave structure provide further evidence for this early observation of "turbulent motion" in the atmosphere.

The existence in the atmosphere of laminar structure, or stable layers of large horizontal extent and small vertical depth, has received attention by several authors. Scorer (1951) noted earlier studies by Taylor and Goldstein (1931) on waves in a fluid of several homogeneous layers and concluded that the meteorological literature had failed to notice the studies because of the

mathematical difficulties and incompletness of their conclusions. Scorer discussed some of the ways in which static stability and shear affect internal gravity (buoyancy) wave properties of an air current and concluded that they play an important part in determining whether or not waves of certain lengths are initially unstable and, if so, to what extent. Danielsen (1959) produced a study which pointed out the failure of researchers to recognize the existence of many zones of large hydrostatic stability often separated by zones of neutral stability. The zones of large stability have spatial and temporal continuity of large horizontal extent and small vertical dimension. The source of this oversight was traced to the processing techniques used on the original radiosonde data. When the original records were reprocessed to show the detailed structure data, many stable layers originally averaged out by the conventional processing techniques were revealed. Danielsen concluded that the mesoscale structure is characterized by many variations in stability and baroclinity that are organized to form isentropic stable laminae in the troposphere and stratosphere. The same laminae may extend from the troposphere into the stratosphere, such that flow from one region to the other is not restricted by a discontinuous surface (tropopause).

Kuettner (1959) reported in some detail on the "streaky parallel trains of clouds" noted by Helmholz. The cloud streets, as Kuettner referred to them, appear to line up in the flow direction and originate in convective layers. The corresponding mean wind profile in the vertical has a jet-like curvature. The resulting wave structure, or actually a helicance-type structure of oppositely directed or paired longitudinal vortices, is reflected in the horizontal and vertical component of wind flow plus the large horizontal and small vertical extent of the cloud streets. An analogous helicance structure was observed during a series of laboratory experiments by Avsec (1939). Conover (1960) reported on extensive observations of cloud band structure and related aircraft measurements of air flow and concluded that the bands are created by parallel horizontal vortices through which air flows in a helical motion.

Kao and Neiburger (1959) noted that air particle trajectories in the horizontal flow field generally depend on the interactions between inertial oscillations and the forcing function of the pressure field. Where the frequency of the inertial oscillation is equal to that of the forcing function, a resonance phenomenon occurs. Newton (1959) observed that the ageostrophic oscillations could arise either from a disturbance of the pressure field or through a disturbance of the wind independently of the pressure field. Sawyer (1961) conducted a study of quasi-periodic wind variations in the lower stratosphere using

radarsonde theodolite data and observed that the atmospheric disturbances had a vertical dimension of approximately 1 km, but horizontal dimensions of perhaps several hundred kilometers. He used perturbation theory to show that inertial oscillations might have such dimensions. Weinstein and Reiter (1965) reported on similar detailed wind profile measurements and concluded that in the presence of geostrophic wind shear, overall thermal stability, and low turbulence energy normally found in the stratosphere, inertial-type oscillations -- once started through a deep layer -- would soon disperse into a series of shallow individual oscillations of different wavelengths capable of maintaining themselves for long periods of time.

Buoyancy-driven or internal gravity waves[1] in the atmosphere have been the subject of considerable study by Hines (1960); Newell, Mahoney, and Lenhard (1966); Hines and Reddy (1967); Gossard, Richter, and Atlas (1970); Jordan (1972); Jones and Houghton (1972); Whitten and Riejel (1973); Duffy (1974); Curry and Murty (1974); Hooke and Hardy (1975); and Gossard and Hooke (1975). Theoretical models have been compared with observations. However, it has been difficult to experimentally obtain the complete atmospheric state and boundary and initial conditions for comparison with theory. In addition, the theory contains many idealizations, not always found in nature, such as horizontal homogeneity, linearization, stationarity of the background flow, etc. Observational evidence indicates that buoyancy waves are always present to some degree when a region of significant stability exists in the troposphere. Generation of buoyancy waves appears to be associated with a variety of sources such as orography, squall lines and frontal systems, shear instability, and wave-wave interactions (Gossard and Hooke, 1975). Direct measurements of mesoscale flow fluctuations in the troposphere and lower stratosphere are limited, although data from a few specific locations are available which have far greater resolution than is permitted by conventional wind profile measurement equipment. This will be discussed further in Section II.

For many years the only way to resolve wave structure in the atmosphere was to use ground-based microbarograph arrays which revealed wave-associated pressure fluctuations (Gossard and Hooke, 1975). This was an indirect technique in the sense that the existence of the wave was inferred from the net

---

1. The phrase "buoyancy waves" is used in preference to the usual phrase "gravity waves" to avoid confusion with gravitational waves predicted by Einstein's general theory of relativity and in accordance with the presentation by Gossard and Hooke (1975).

effect of the wave on the surface pressure field. Danielsen (1959) restudied original rawinsonde data records and developed detailed observational evidence of the tropospheric and lower stratospheric flow structure. Sawyer (1961) produced one of the earlier sets of measurements for the lower stratosphere using a radarsonde theodolite to track a balloon. Miller, Henry, and Rowe (1965) and Manning, Henry, and Miller (1966) used smoke trails observed by cameras to develop detailed vertical and wind profile measurements from near the surface to approximately 30 km altitude. Scoggins (1963) and Fichtl, Camp, and Vaughan (1968) described a radar-balloon technique and the resulting measurements of detailed wind profile structure from the surface to approximately 18 km altitude. DeMandel and Scoggins (1967) noted in a preliminary analysis of these data that significant mesoscale variations in wind speed are common, particularly in and above the region of maximum wind. Gossard, Richter, and Atlas (1970) discussed detailed wind structure measurements acquired by a vertically pointing radar which has both high sensitivity and ultra-high resolution (<1 m). These remotely-sensed very small-scale features, which had not previously been observed, revealed a complex and wide range of wavelengths and frequencies.

The research reported herein originated as part of a National Aeronatuics and Space Administration (NASA) program to develop instrumentation to accurately measure detailed wind profiles. The instrumentation was required to provide measurements of the detailed wind profile structure for the design of space vehicle structures and control systems. (A brief summary of some engineering descriptions of these data is given in Appendix A.) The success of this effort resulted in the accumulation of many troposphere and lower stratosphere detailed wind profile data sets. This led naturally to a more basic inquiry into the behavior and generating mechanisms of mesoscale fluctuations which is the subject of this study.

The research is reported in the following order. Section II gives a description of the measurement system and characteristics of the experimental data. Section III reports on an analysis of the structure and time persistence of the data. Section IV discusses the models and physical mechanisms. Section V gives the conclusions of the investigation.

II. DESCRIPTION OF DATA

The data used in this study consist of several sequences of detailed wind profiles measured by the Jimsphere radar system. The data involve a series of measurements at approximately 2 h intervals made over periods of time up to approximately 18 h. Measurements were made from approximately 200 m altitude to near 18 km altitude, a range that encompasses the troposphere and lower stratosphere. Several sequences of these measurements are shown in Appendix B. The analysis presented in Section III involves three sequences selected to represent typical meteorological conditions.

A. Measurement Method

The wind data utilized in this research were obtained by the Jimsphere radar system. The system consists of a 2 m diameter, "rough," aluminized, Mylar sphere which is tracked by the FPS-16 (or equivalent) high-precision radar. The purpose of the surface roughness elements is to control vortex formation and separation, thus reducing aerodynamically or self-induced balloon motions.

The Jimsphere wind sensor is a spherical, 2 m diameter, 0.5 mil metalized Mylar balloon fabricated from 12 tailored gores. It has 398 protrusions (cones) approximately 0.08 m high which serve as "roughness" elements. The balloon overpressure is maintained at 6 to 8 mb by a helium vent valve. This system has a ballast of 100 gm to retard spin motions, and the complete system weighs 400 gm. The balloon has a mean rise rate of approximately 5 m s^{-1}, and the ceiling height is approximately 18 km.

Smooth spherical balloons that do not have a sufficiently small diameter operate in the supercritical Reynolds number region, Re $\geq$ 3 × 10^5, where Re is a Reynolds number based upon the rise rate and diameter of the balloon. The supercritical Re region for a sphere is characterized by low values in the drag coefficient (C_D) as shown by the smooth sphere wind tunnel data (Schlichting, 1960) in Figure 1. The wake associated with a smooth sphere in the supercritical Re region is unstable, and this instability results in random lateral fluctuating lift forces with no preferred periods of oscillation. These

6
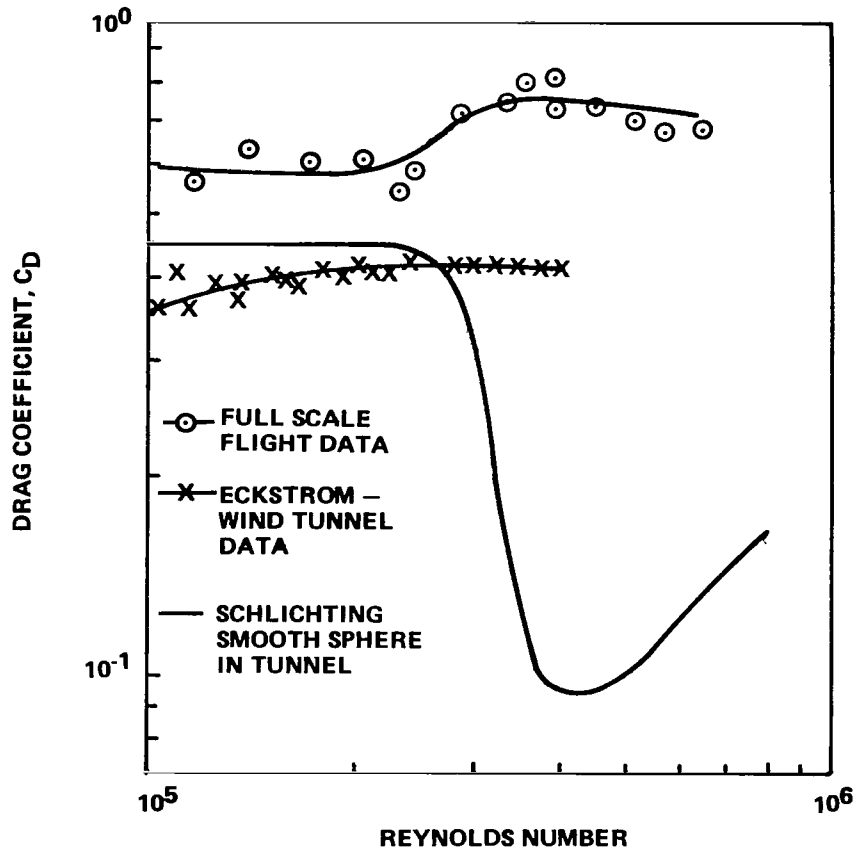
Figure 1. Drag coefficient data.

forces cause the balloon to execute spurious motions as it ascends through the atmosphere and thus contaminates the wind profile measurements.

Random balloon motions can be eliminated by stabilizing the wake behind the balloon. This can be accomplished by increasing the C_D, and thus drag, through a reduction in the Re so that the balloon will operate in the subcritical Re region ($Re < 3 \times 10^5$). The Re can be reduced in two ways. One way is to reduce the diameter of the spherical balloon; however, this would result in a reduction of the lift forces and thus a reduction in the rise rate. ˙ The second way is to keep the diameter of the balloon fixed and introduce an additional length scale, so that the effective length scale of the system is smaller than the diameter. In the case of the Jimsphere balloon, the conical protrusions serve

7

this purpose by organizing the vortex shedding into stable modes. The question concerning the selection of a proper length scale for calculating an Re has yet to be answered. However, the important point is that the addition of conical elements to a smooth balloon causes C_D to increase in the supercritical Re region and results in the desired stabilized wake. Full-scale wind flight test data for the Jimsphere configuration are shown in Figure 1 (Scoggins, 1967). This figure shows clearly that the conical protrusions produce an increase in the C_D in the supercritical Re region of the smooth balloon configuration. The Eckstrom (1965) wind tunnel Jimsphere model was approximately 13 cm in diameter. The full-scale C_D are larger than the wind tunnel values. The difference is attributed to the fact that in the full-scale tests the balloon was free to move, while the wind tunnel model was held fixed during the tests.

It is important to note that the conical elements on the Jimsphere do eliminate the spurious balloon motions. However, the Jimsphere balloon executes a regular self-induced balloon motion. Rogers and Camitz (1965) performed a study of the self-induced motions of the Jimsphere using Doppler radar. They found that the Jimsphere experiences a periodic helical motion with a period of 4.5 s, which corresponds to a vertical wavelength of approximately 25 m. No other significant spurious motions were observed. This orderly self-induced balloon motion is easily removed from the data because it is an extremely narrow band process.

According to Rogers and Camitz, the data reduction method developed by Scoggins (1963) essentially eliminates the observed spurious motions. In this procedure the position coordinates, which are sampled by radar at 0.1 s intervals, are averaged over a period of 4 s centered on 25 m altitude intervals. Finite differencing over 25 m altitude intervals then gives wind velocities which, although computed for each 25 m, represent averages over an altitude interval of approximately 50 m.

Scoggins and Susko (1965), Scoggins (1965), and Susko and Vaughan (1968), by using two radars to track one Jimsphere, have shown that wind speed measured by this method has an rms error generally less than 0.5 m s^{-1}; wind direction is measured with an rms error of no more than 1 or 2 degrees. These measurements are at least one order of magnitude more accurate than measurements made by the rawinsonde system. Thus, it is now possible to investigate tropospheric and lower stratospheric mesoscale motions on a routine and consistent basis.

B. Specific Characteristics

The most significant features of the wind profile are wind speed and direction fluctuations which persist, often throughout the whole sequence of measurements at approximately the same altitude. Appendix B provides a sample selection of the detailed wind profiles used in this research. One way of viewing the nature and characteristics of these fluctuations is by considering perturbations about a mean wind profile which should remain constant — or nearly constant — throughout the period of observation. Even a brief review of the profiles given in Appendix B reveals an impressive variety of scales of wind flow perturbations that may exist in the atmosphere and their persistence or lack of persistence. Specifically, the following categories of wind speed perturbations may be recognized:

1. Macroscale (jet stream) perturbations having a vertical wavelength generally greater than approximately 10 km and an amplitude greater than 20 m s^{-1}, and usually persisting unchanged through the series. (The sequence of profiles shown in Figure B-1 of Appendix B is a good example.)

2. Mesoscale perturbations having a vertical wavelength from approximately 1 to 3 km and an amplitude up to approximately 15 m s^{-1}. Individual wind speed maximums from these perturbations persist from several hours to a time period longer than that over which the sequential measurements were taken. Often the amplitude and occasionally the vertical wavelength of the perturbations change considerably from one profile to the next such that successive perturbations are not exact replicas of each other, yet can still be rather easily identified as the same feature. (The sequence of profiles shown in Figure B-2 of Appendix B is an excellent example of these features.)

3. Microscale (turbulence) perturbations having a vertical wavelength less than approximately 1500 m and an amplitude up to approximately 6 m s^{-1}. These oscillations differ from the small mesoscale features principally because of their highly transient nature. They are common perturbations on a given profile but lack continuity in time. (The profiles given in Figure B-3 of Appendix B demonstrate the turbulent perturbations.)

Several examples of individual wind profiles may help in developing a frame of reference for specific wind profile features such as (1) jet stream winds, (2) sinusoidal variation in wind with altitude, (3) high winds over a
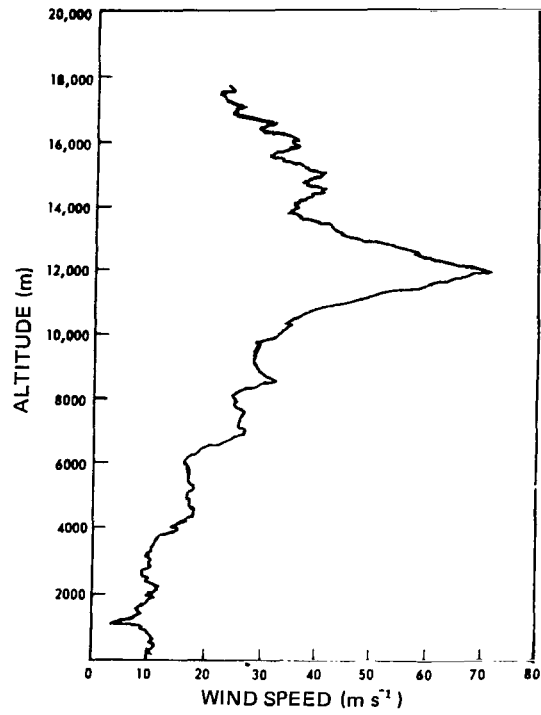
Figure 2. Jet stream wind profile.
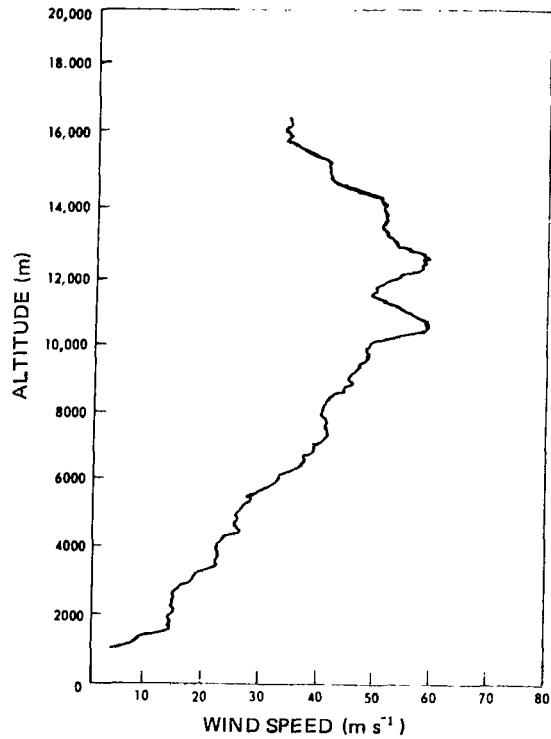
Figure 3. Sinusoidal flow pattern.

broad altitude range, (4) light winds throughout the troposphere, and (5) dis-crete gusts. Jet stream winds (Fig. 2) are quite common during the winter months and can reach magnitudes in excess of 100 m s^{-1}. These winds often occur over a limited altitude range and produce large wind shears over several kilometers. Directional variations in the profile are usually at a minimum. Figure 3 depicts a wind profile with sinusoidal behavior. These mesoscale sinusoidal features vary in amplitude, wavelength, and cycles. They are especially noticeable in the portion of the wind profile measurements that extend into the relatively stable layered structure of the stratosphere where the persistence of buoyancy and inertial waves is most evident. Figure 4 pre-sents an excellent example of high winds over a large altitude range. Notice that the wind speeds exceeded 50 m s^{-1} for over 10 km in altitude. Figure 5 shows a wind profile with speeds less than 15 m s^{-1} and is typical of the summer season. Figures 6 and 7 illustrate two examples of single discrete mesoscale perturbations that may occur at any altitude and speed of the wind profile.
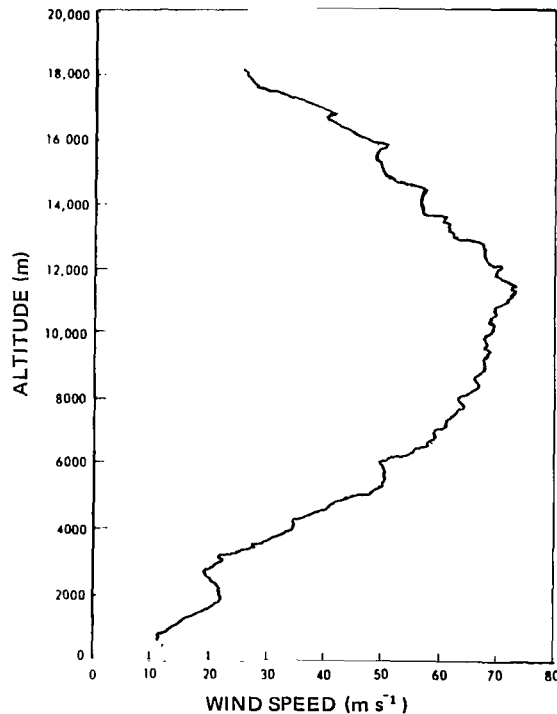
Figure 4. High wind speeds over deep altitude layer (jet stream flow).
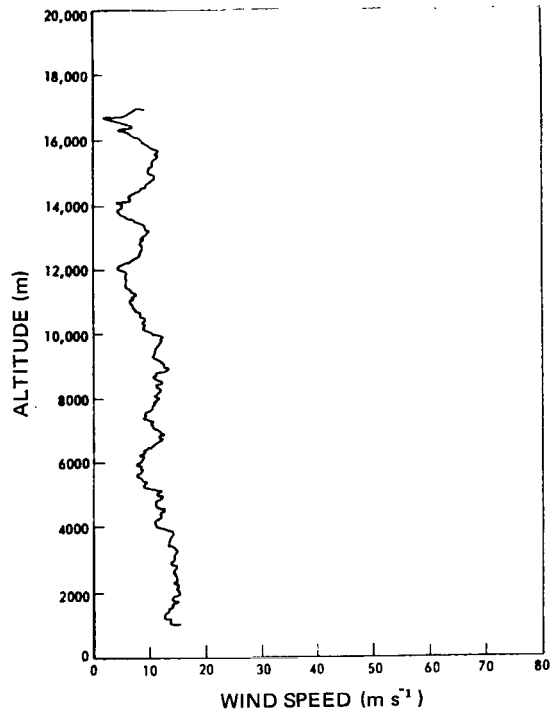
Figure 5. Low wind speed profile.
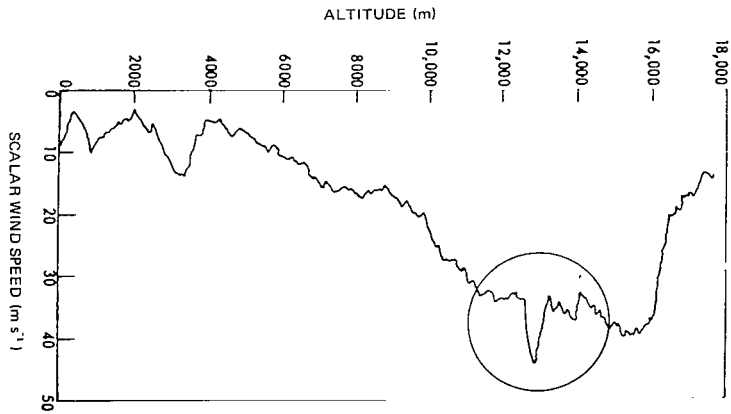
Figure 6. Triangular wave shape of discrete mesoscale perturbation.
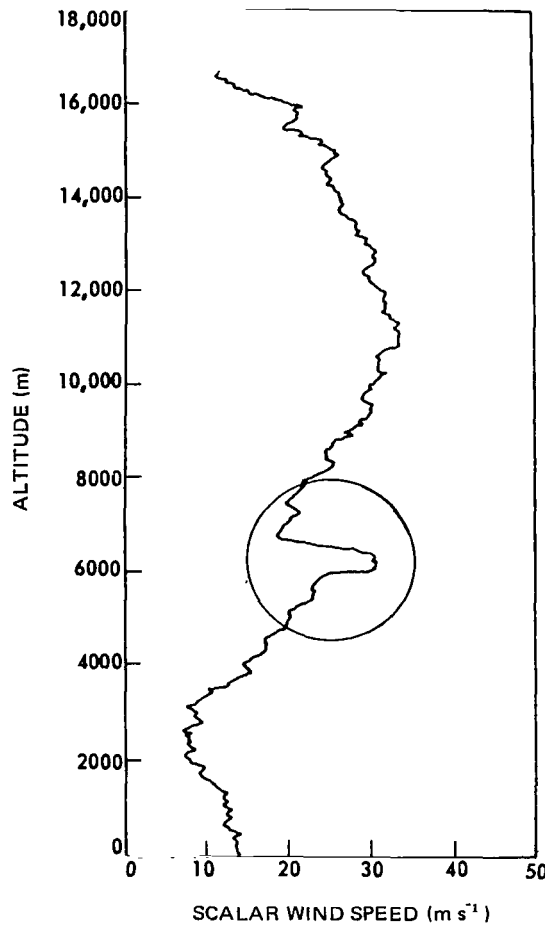
Figure 7. Quasi-square wave shape of discrete
mesoscale perturbation.

Although three categories of wind speed perturbations were identified
earlier in this section, it should be noted that the spectral analysis of the data
which is presented in Section III did not show any preferred wave numbers that
correspond to the macroscale, mesoscale, or microscale terminology. There
appears to be no clear-cut, natural separation between the different scales of
motion in the free atmosphere as revealed by vertical wind profile measure-
ments. Instead, as far as spectrum shape is concerned, divisions between
vertical scales or categories may be selected arbitrarily. However, the energy
of the atmosphere is not spread uniformly over all wave numbers when horizontal
wind measurements at a fixed height are analyzed but has certain preferred

scales, with gaps in between, according to Fredler and Panofsky (1970). It appears that atmospheric scales can best be determined by reference to horizontal observations of the wind flow.

The mesoscale category of wind speed perturbations has a significant interest to engineering and scientific studies. Figure 8 provides an example of some common changes in mesoscale perturbations. The uppermost sequence of data illustrates an unsteady growth and decay of mesoscale perturbations. The middle sequence of data shows a steady growth of a prominent mesoscale feature. The lower sequence of data provides an excellent example of a splitting process occurring in a mesoscale perturbation with the primary peak maintaining itself throughout the 12 h sequence at approximately 16.5 km altitude. Appendix B contains several plots of wind speed sequences for various mesoscale flow perturbations. They are representative of the data measured by the Jimsphere radar system which were used in this research effort. Johnson and Alexander (1976) have presented graphical data on a large number of sequential Jimsphere radar detailed wind profile measurements which further illustrate the characteristics discussed herein.

III. ANALYSIS OF STRUCTURE AND PERSISTENCE

A. Introduction

The rather interesting structure and persistence of mesoscale perturbations in vertical detailed wind profiles are evident from an examination of the data given in Appendix B. This analysis is based on computations by Endlick, et al. (1969) and is concerned with the spectral distribution of wind variations measured along paths that, for purposes of this study, are considered to be essentially vertical (true only if the mean wind velocity is constant with height). Also, the time difference of approximately 1 h between the beginning and end of a Jimsphere balloon flight is ignored. Neither of these conditions is believed to restrict the analysis and conclusions. Much previous work has been done using spectral analysis of detailed meteorological data, particularly those data obtained on towers (Lumley and Panofsky, 1964). In the free atmosphere, spectral computations have been applied to aircraft measurements of small-scale, three-dimensional turbulence in the lower end of the inertial subrange
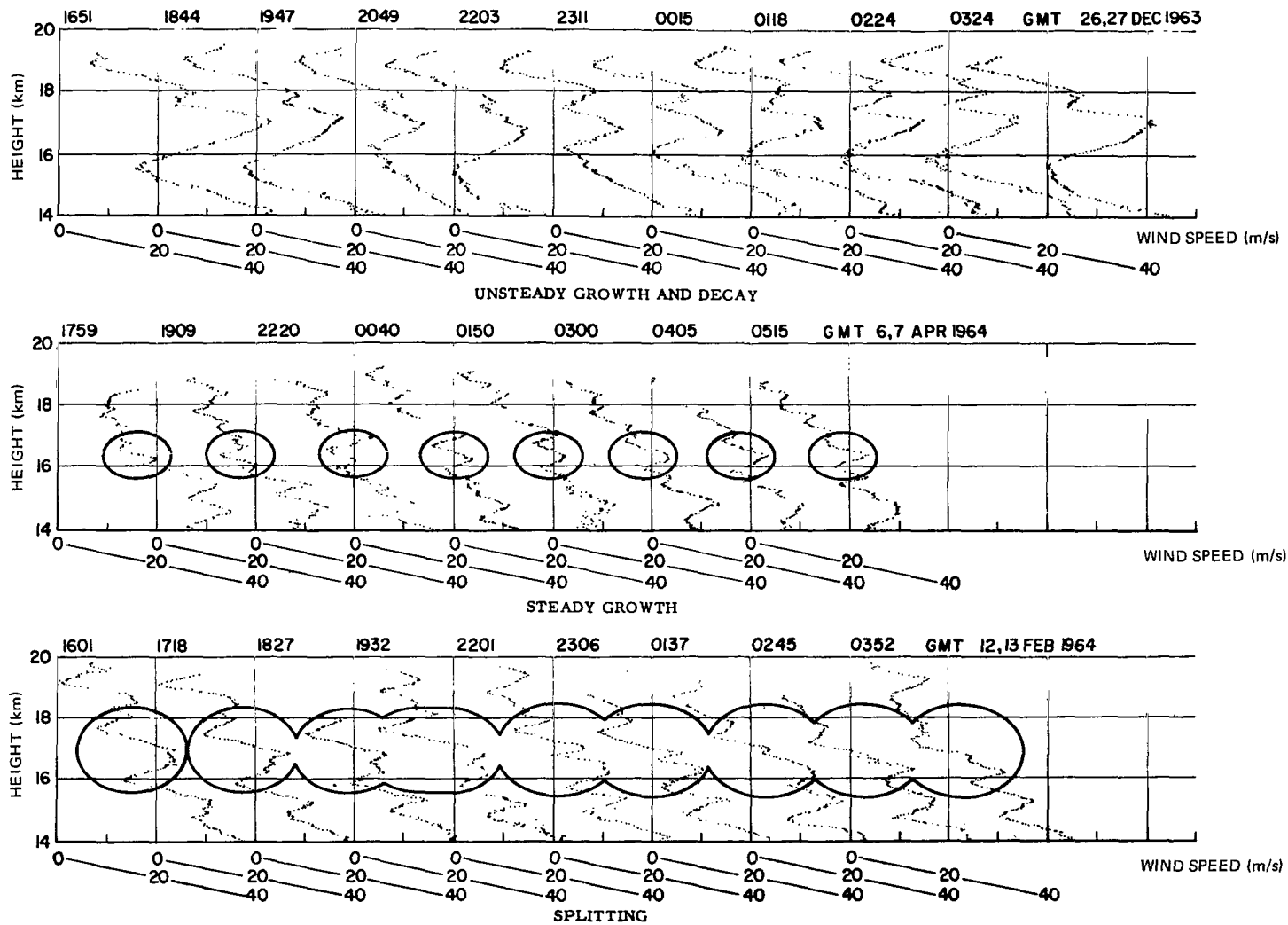
Figure 8.   Common changes in mesoscale perturbations.

and its extension into the wave number region of the energy-containing eddies. At these scales it is well known that turbulent eddy kinetic energy decreases with wave number according to the -5/3 power law.

The detailed wind profiles generally cover heights from approximately 0.2 to 18 km. Within this distance the winds may increase to jet stream speeds at 10 to 12 km and then decrease again to low speeds in the stratosphere. The same variation of winds occurs only in much greater horizontal distances, on the order of several hundreds of kilometers across a jet stream, or of a thousand kilometers or more along a jet. This difference in scale makes it interesting to compare spectra of winds from rising balloons to previous spectra along horizontal lines as given, for example, by Pinus (1963), Kao and Woods (1964), Pinus et al. (1967), and Vinnichenko and Dutton (1969). This comparison is shown later in Section III. E.

B. Computations

Digital spectral analysis was used to determine the distribution of the power (or energy) of the wind speed variations along a vertical axis. Power spectral analysis was performed on each profile. Average results of these spectral computations were obtained visually for each sequence and are shown in Section III. C.

The detailed wind profile data were processed at each 25 m height over a layer 50 m in depth; therefore, the highest wave number contained is 10 cycles km^{-1}, corresponding to a 100 m wavelength. The roll-off of the filter used in the processing is such that one gets approximately 90 percent of the energy at a 100 m wavelength (DeMandel and Krivo, 1971). Three sequences of wind speed profiles from Cape Kennedy, Florida, were examined in detail. Each sequence contains four or more profiles measured at 1 to 2 h intervals. One sequence in April shows a typical jet stream profile; the second in July appears typical of weak summertime flow; and the third in November has intermediate speeds with more jaggedness, suggesting prevalent mesoscale features. These profiles are shown graphically in Section III. C. Since the wind speeds are at 25 m intervals from the surface to approximately 20 km in altitude, the wave number range of the spectral analysis of the profiles is from 0.05 (actual information cutoff is at approximately 0.07 cycle km^{-1}) to 10 cycles km^{-1} (corresponding to wavelengths of 20 km to 100 m).

The method of data processing of the wind data used in this study has been described by Scoggins and Susko (1965). The zonal and meridional components of wind are averages over a layer approximately 50 m in depth and are given at 25 m height intervals. Thus, the aerodynamic balloon motions and any atmospheric eddies smaller than approximately 100 m have been eliminated to a large degree. However, a few spurious points, mostly false speed maxima or minima, were encountered in the wind profiles. These were eliminated by a subprogram that tested the difference between successive points on the wind profile. If this difference (in either speed component) was larger than a critical value, an interpolated point was substituted for the erroneous one. The critical value was taken as 4 m s^{-1} for strong wind profiles and as low as 2.5 m s^{-1} for cases of weak winds (based upon experience gained from study of many individual profiles). Experimentation showed that the high wave number end of a spectrum plot was significantly raised if even a few spurious spikes were included; thus, the matter is of practical importance.

The wind data generally began approximately 200 m above sea level and terminated at an altitude between 15 and 18 km. In studying a given sequence of Jimsphere radar measurements, all profiles were terminated at the lowest upper limit so that each profile of the sequence would cover exactly the same altitude range.

A basic assumption in spectral analysis is that the data sample interval spans one period of a periodic function; i.e., the final point of the sounding is followed by the first point and then by the rest of the record, ad infinitum. If the values of the first and last points are nearly the same, only a small discontinuity in shape is implied if they are effectively made adjacent to each other. However, in the present data, the differences between the speeds of the first and last points were sometimes large. To avoid a discontinuity in shape and the associated effects of added high wave number power in the spectrum, a smooth, cosine-shaped connection was inserted between the last measured point and the first point. The first point of the profile was assumed to occur again at 20.5 km, and the cosine connection was made between the last point (e.g. 16 km) and this repeated value. (An example is shown in the smooth, upper portion of curve g in Figure 9.) Comparisons between actual spectra computed with and without the cosine connection showed its effectiveness in portraying accurately the higher wave numbers.
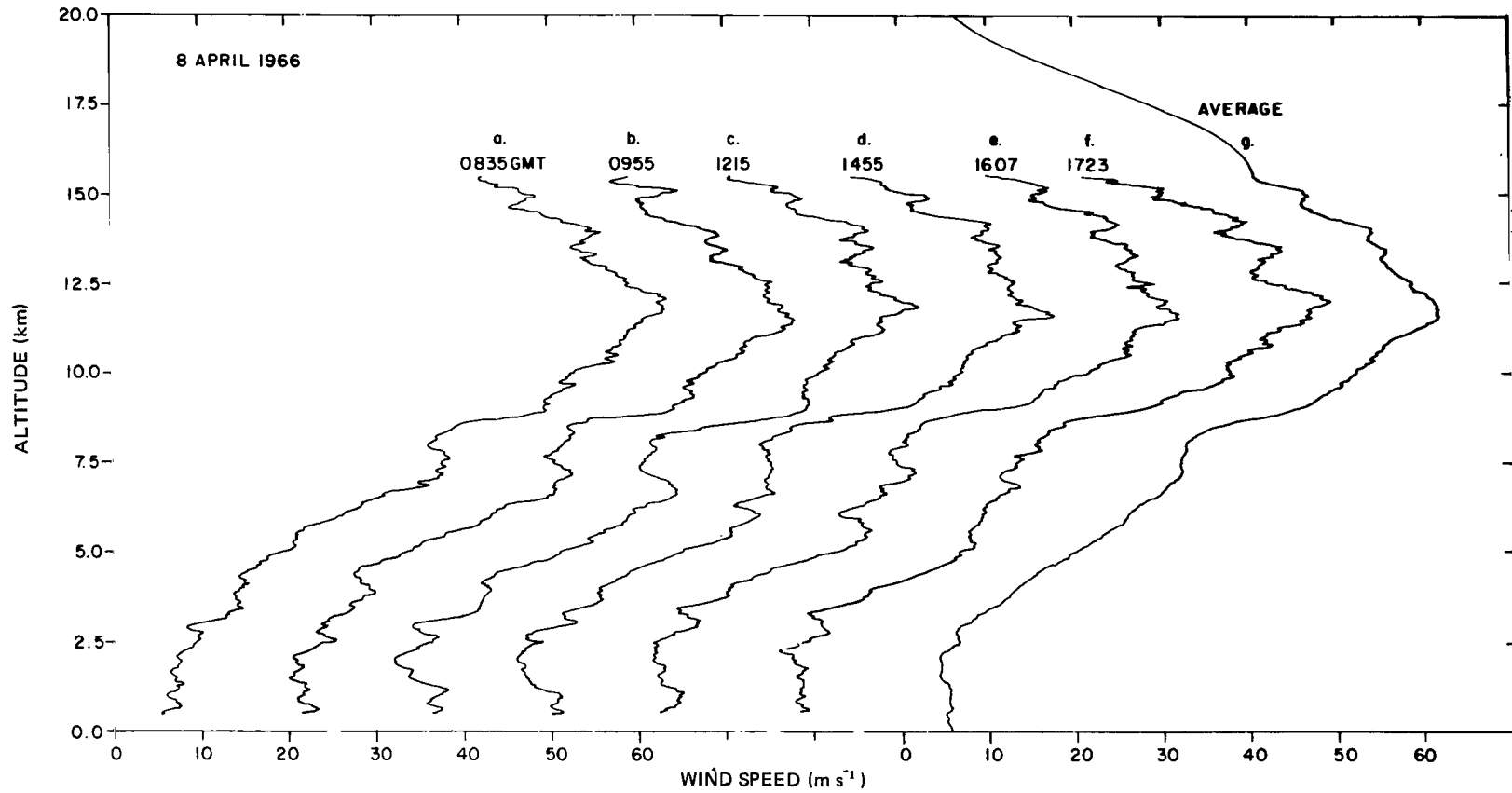
17

Figure 9. Sequential wind speed profiles measured at Cape Kennedy, April 8, 1966 (the speed scale is shown only for profiles a and g).

Statistical homogeneity along the mean balloon tracks is assumed for purposes of this spectral analysis of the detailed wind profile structure. If the ensemble of wind profiles has statistical homogeneous properties, then the spectrum of the wind profile is real and independent of position or height. For the purposes of this analysis, this assumption is not a limiting factor. However, in reality, an ensemble of wind profiles is not statistically homogeneous. This has been discussed in some detail by Fichtl (1972). One example of the non-homogeneous behavior of wind profiles is the general increase and decrease of the wind speed below and above the core of an atmospheric jet stream. A second example is the change in the wind perturbation structure as height increases through the troposphere; i.e., the wind perturbations above the mean wind profile which extends above the tropopause (~10 to 12 km altitude) tend to be larger than the ones below the tropopause, especially when the troposphere is convectively unstable. Appendix B contains several examples of this feature. Gravity wave theory provides a third example. According to Hines (1960), the buoyancy or gravity waves produce wind perturbations which have Fourier amplitudes that increase with altitude like exp $(Z/2H)$, where Z is altitude and H is the atmospheric scale height:

$$H = \left(\frac{1}{\rho_o} \frac{\partial \rho}{\partial Z} \right)^{-1} \quad ,$$

where ρ is the atmospheric density, thus rendering the process nonhomogeneous.

C. Sequential Data Set Analysis

1. <u>April Sequence of Wind Speed Profiles</u>. The wind profiles measured on April 8, 1966, at Cape Kennedy, Florida, during the period 0835 to 1723 GMT are shown in Figure 9. The profiles were measured in a uniform westerly, upper-air flow. All have maximum speeds slightly greater than 60 m s^{-1}. The profile shapes are similar relative to the macroscale, but rather large differences between the profiles can be noted in the more detailed mesoscale and microscale features.

Before proceeding to a presentation and discussion of the results obtained in terms of the averaged spectra, it is worthwhile to mention some of the characteristics observed in the power spectral density calculations for the

individual profiles. As expected, the power spectral densities of the individual wind speed profiles decreased rapidly with increasing wave number. The steepest decline occurred at a wave number of approximately 0.2 cycle km^{-1}, where the logarithmic plots of the data showed the slopes to be nearly –8. At wave numbers above approximately 0.5 cycle km^{-1}, the spectra were characterized by slopes close to –2.5. Differences between the spectra appeared to be random and are due to differences in the detailed features of the wind profiles shown in Figure 9. It is interesting to note that a line with a slope of –5/3, which applies to turbulence in the inertial subrange (Hinze, 1975), did not possess sufficient slope to be steep enough to fit any portion of the spectra. However, it should be noted that if one invokes the theory of a buoyancy subrange, for which a spectral slope of –3 is predicted (Lumley, 1964), then closer agreement with the –2.5 slope is obtained. The spectral region associated with a buoyancy subrange is controlled by the Väisälä-Brunt frequency as opposed to the inertial subrange which is controlled by the viscous dissipation rate of turbulent kinetic energy. Invoking the concept of a buoyant subrange is not an unreasonable speculation and implies that the detailed wind profile structure with a wavelength less than approximately 500 m may be a gravity wave related phenomenon. Spectra were computed also for individual meridional and zonal wind component profiles. These were very similar to the spectra of the speed profiles except that the meridional components contained less energy at low wave numbers. This was due to the relatively small meridional component magnitudes in this case of predominately westerly winds.

Another way to investigate the scales of variability of these wind profiles is to compute an average profile and the deviation of each individual profile from the average. The ensemble average speed at each 25 m height increment was determined simply as the mean of the six individual speed profiles at the same height. The profile of these averages together with the cosine connection is shown in curve g of Figure 9. This curve is smoother than the individual profiles but otherwise resembles them closely because the macroscale patterns were not changing rapidly. A very interesting feature of this sequence is that even the average profile shows mesoscale wave structure. This implies a time scale larger than the sequence which encompassed a period of 9 h.

The individual profiles of the deviations from the mean are shown in Figure 10. Each has some similarities and some differences from its neighbors. Some features, such as the relative maximum at 3 km altitude in the last three profiles, persist almost unchanged for 4 h; others, such as the wind speed maximum at 8.5 km altitude at 1215 GMT, do not persist. The average spectra were
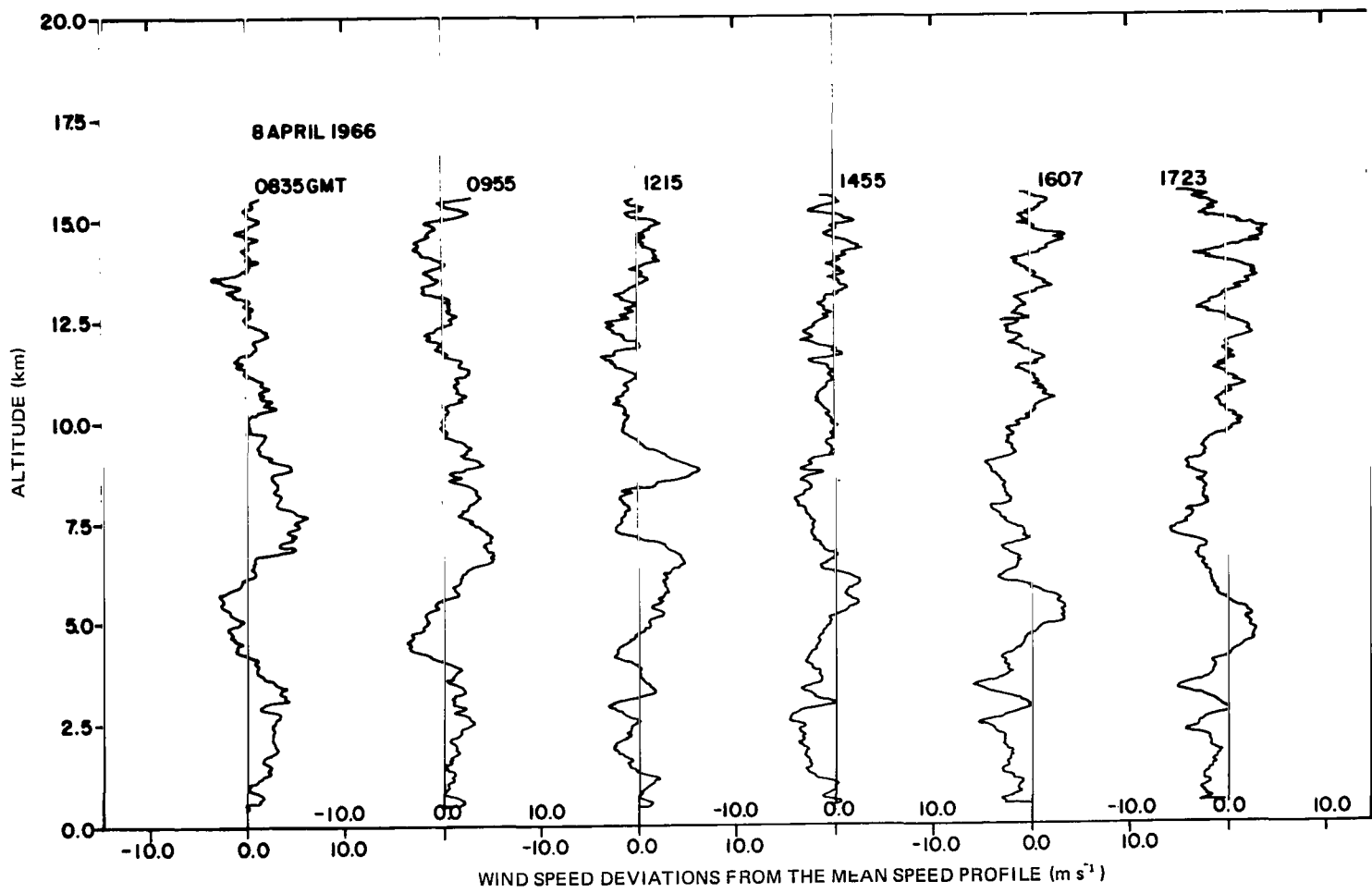
Figure 10. Deviation of individual wind speed profiles from the mean profile, April 8, 1966.

computed to determine information on any predominant wave numbers. These results will be discussed later, but some features of the spectra for the individual speed deviation profiles used in the computations were of interest. The spectra tended to flatten at wave numbers less than 0.5 cycle km^{-1} because the larger wavelengths were essentially relegated to the mean profile which was removed by subtraction. The wave numbers higher than 1 cycle km^{-1} has a slope near -2.5 with no consistent gaps. Differences between the spectra of the individual deviation profiles shown in Figure 10 were largest at wave numbers from 0.3 to 1.0 cycle km^{-1}.

A further interesting comparison of the wind profiles comes from taking the differences between profiles. One may inquire whether changes to be expected in a few hours are similar to those changes that have occurred in previous hours. Changes between successive profiles are shown in Figure 11. (Note that the time intervals are not uniform, but vary from 1 h, 20 min to 2 h, 40 min.) The change profiles have general characteristics similar to the deviation profiles of Figure 10. Consistency of appearance between the change profiles is not very great. Of course, a relatively high speed in one profile of Figure 9 at a given altitude will appear as a maximum at that altitude in one speed-change profile and as a minimum point in the following speed-change profile. The spectra of the five profiles of speed changes were similar to the spectra of deviations from the mean profiles except that they contained somewhat greater energy at higher wave numbers.

To compare the different types of spectra, the individual spectra for the speed profiles shown in Figure 9 were drawn on a single graph, and a smooth curve was visually fitted to them to produce an average. This curve is identified as the "smoothed spectrum of individual wind speed profiles" in Figure 12. Two other smoothed curves were prepared from spectra for the individual wind speed deviation profiles in Figure 10 and spectra for the individual wind speed change profiles in Figure 11; these are denoted as the "smoothed spectrum of speed deviations" and the "smoothed spectrum of speed changes" in Figure 12. Also, a visually smoothed version of the spectrum of Figure 9 (curve g) is called the "smoothed spectrum of the mean speed profile."

Curve A in Figure 12, the "smoothed spectrum of individual speed profiles," has a relative minimum (in terms of deviation from the -3 line) at vertical wavelengths between approximately 1 and 3 km. This was mentioned earlier in regard to the individual profile spectra. Since this region is often referred to as mesoscale, there seems to be considerable doubt that mesoscale
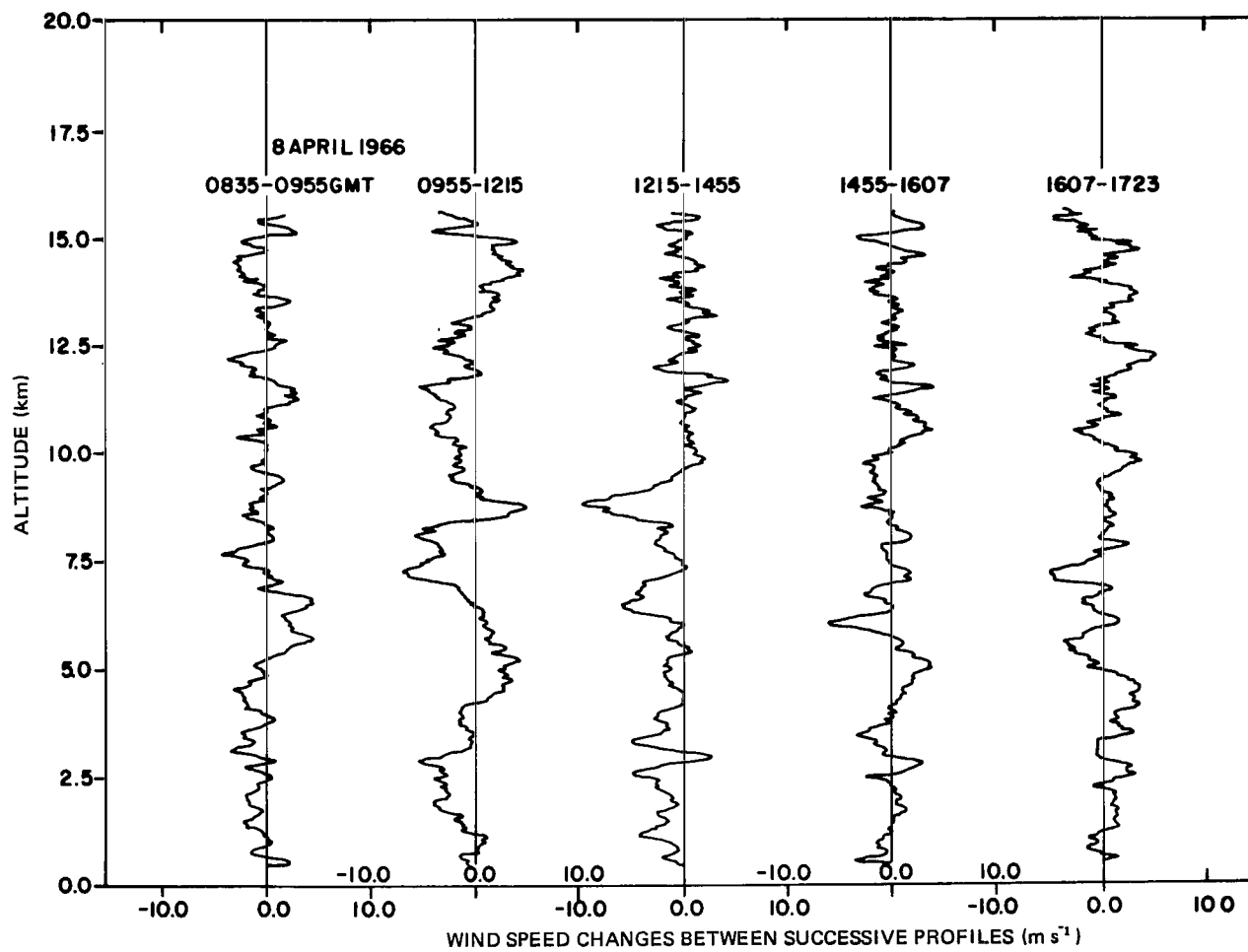
Figure 11. Speed changes between successive profiles, April 8, 1966.
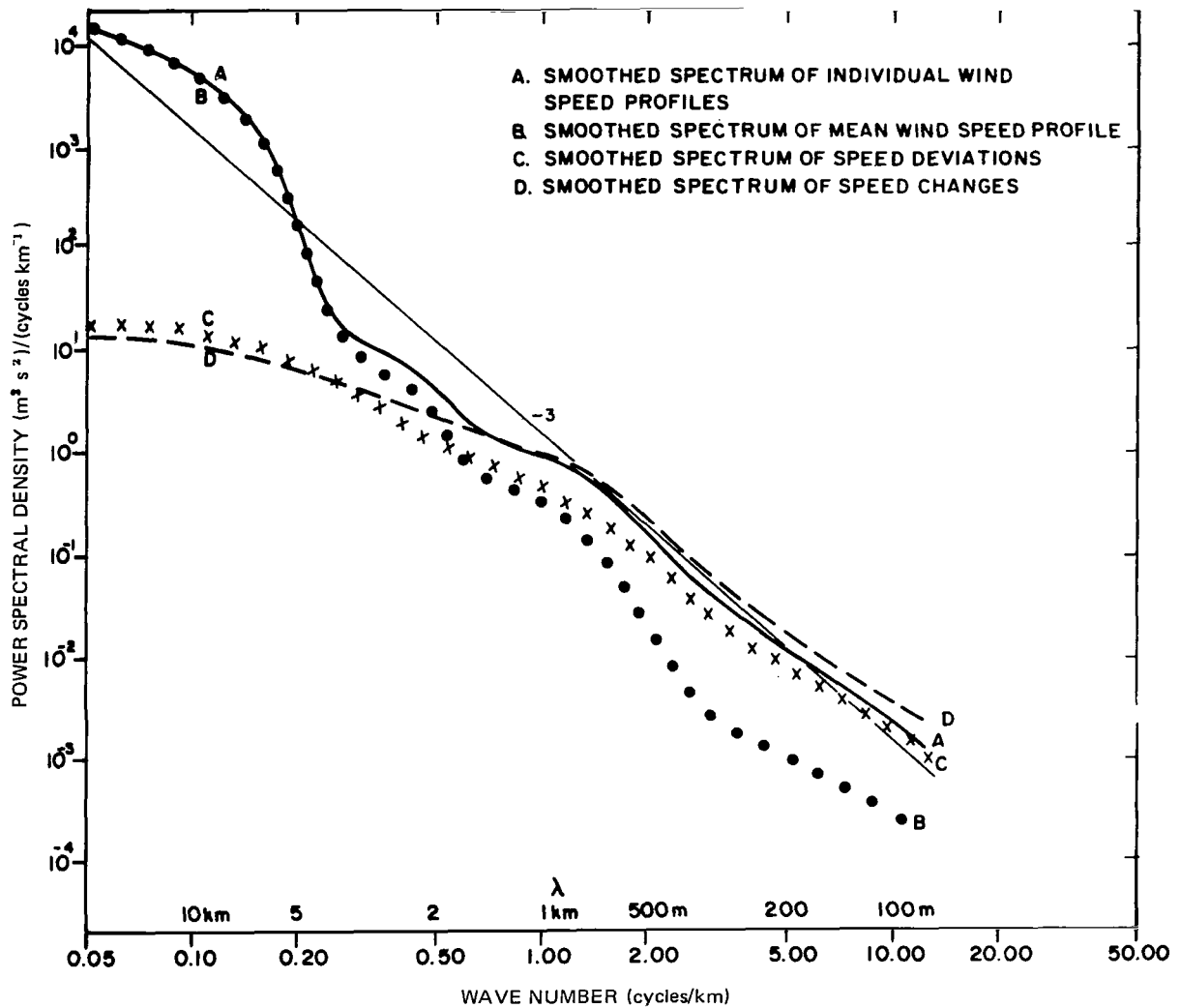
Figure 12. Summary of spectra of wind speed profiles,
April 8, 1966.

eddies in these vertical profiles are independent characteristics. Although one
can certainly identify maxima and minima in layers 1 to 3 km deep in the pro-
files of Figure 9, such features are evidently the combined effects of a variety
of wavelengths in the spectrum rather than the result of a predominant scale.
This result may be taken as a warning against making interpretations of scales
of motion by simple visual inspection of complex wind profiles.

The "smoothed spectrum of the mean profile" (curve B in Fig. 12) departs from curve A at a wavelength of approximately 4 km and then conforms roughly to a -3 slope with some rather minor deviations. Curve C, the "smoothed spectrum of speed deviations," lies between the two spectra discussed previously and has a smooth shape with only small high and low points. If it were possible to forecast the mean wind speed profile (curve g in Fig. 9) but not the deviations, then curve C would represent the spectral distribution of errors. Note that curve C intersects curve B at a wavelength of approximately 2 km, where the mean and deviation profiles contribute equally to the variance. The "smoothed spectrum of speed change," curve D in Figure 12, lies approximately a factor of two above the other spectra at the high wave number end of the spectrum. This implies that the microscale features of successive profiles are basically uncorrelated. Also note that curve D intersects curve C at a wavelength of approximately 3 km; at longer wavelengths it has slightly lower power than curve C. Curve D can be interpreted as the spectrum of the errors of a pure persistence forecast of the wind profile; i.e., if a detailed wind profile measured 1 or 2 h before launch is input to the guidance system of a space vehicle, then the resulting changes will be errors having the statistical properties of curve D.

These spectral relationships apply only to the particular synoptic situation of April 8, 1966; therefore, other cases must be investigated to examine the generality of these findings. Two of these are discussed in the following sections. However, although the general conclusions relative to the qualitative aspects are probably universal, other cases would be needed to determine quantitative departures or differences.

2. July Sequence of Wind Speed Profiles. A July sequence was selected to represent summer conditions when wind speeds are typically weaker than in winter. Six profiles were measured at 2321 GMT on July 4, 1966, and between 0040 and 0930 GMT on July 5, 1966. Thus the measurements were made at intervals of approximately 2 to 2.5 h. The synoptic situation consisted of a weak high-pressure area at sea level over Florida, with westerly winds aloft.

The individual wind speed profiles are shown in Figure 13. The first profile of the series is anomalous, in terms of having small, irregular microscale shears throughout. These do not appear in the other profiles of the sequence; perhaps they may be attributed to some equipment difficulty. The speed maximum located at approximately 13 km in curve a of Figure 13
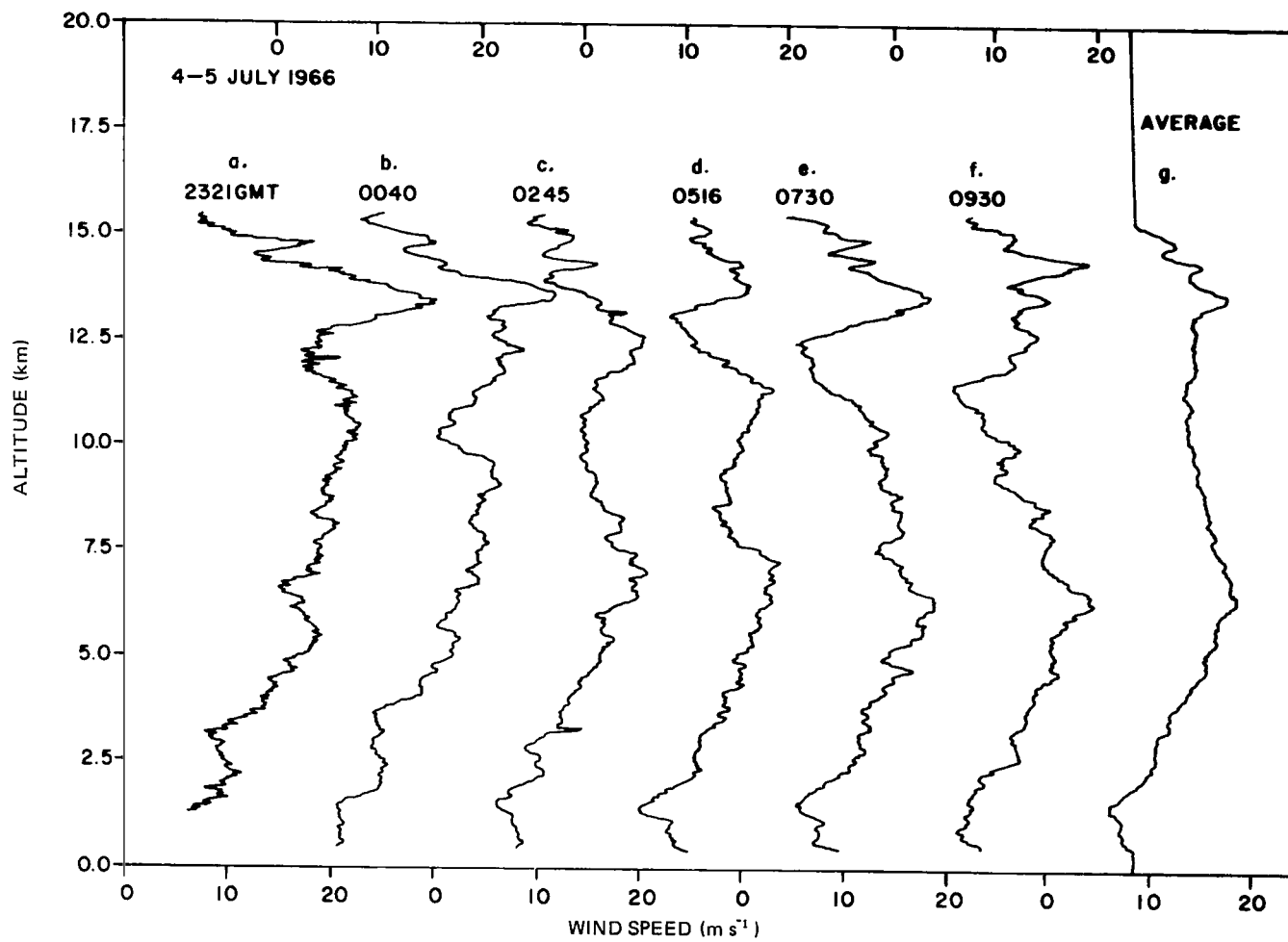
Figure 13. Sequential wind speed profiles measured at Cape Kennedy,
July 4-5, 1966.

decreases in magnitude by the time of curve c and is found at progressively lower and higher altitudes in later profiles. As in the April sequence of profiles, there are some features that persist from one profile to the next of Figure 13, especially if altitude changes and other features that change erratically are permitted. The mean speed profile for this series (excluding profile a) is shown as curve g in Figure 13, together with the cosine connection above approximately 15 km.

The spectra of the individual speed profiles departed strongly from a −3 line at wave numbers above 5 cycles km^{-1}; evidently, this was due to the speed variations mentioned in the preceding paragraph. On an overall basis, the spectra of the July individual speed profiles conformed to the −3 line reasonably well and, thus, had slopes similar to those found in April; however, the July winds are of lower speeds and the spectra contained less total variance.

Deviations of the individual profiles from the mean are shown in Figure 14. Below approximately 7.5 km the deviations are relatively small; however, at higher altitudes they are as large as those observed in the April data (Fig. 10). In Figure 14 a rather marked minimum in speed appears at approximately 14 km in the deviation profile for 0245 GMT. This feature then appears at successively lower altitudes as time proceeds. Most other features have less persistence.

The spectra of the individual deviation profiles were very similar to those for the April series and contained as much or slightly more variance. The higher wave numbers conformed to a slope of approximately −2.5.

The changes in speed between profiles are shown in Figure 15. These changes, like those of the deviations in Figure 14, have largest magnitudes in the upper troposphere. Here the patterns tend to persist if one allows for vertical displacements. The individual spectra of the July speed change profiles were similar to those of the April series.

A smoothed spectrum representing the spectra of the individual profiles shown in Figure 13 is labeled A in Figure 16. It was prepared in the same manner as curve A in Figure 12. Similarly, the other curves in Figure 16 represent the mean profile (curve B), the deviations from the mean (curve C), and the changes (curve D). In Figure 16 their relative characteristics can be compared. Crossing points between curves A and D and between B and C are at lower wave numbers than in Figure 12.
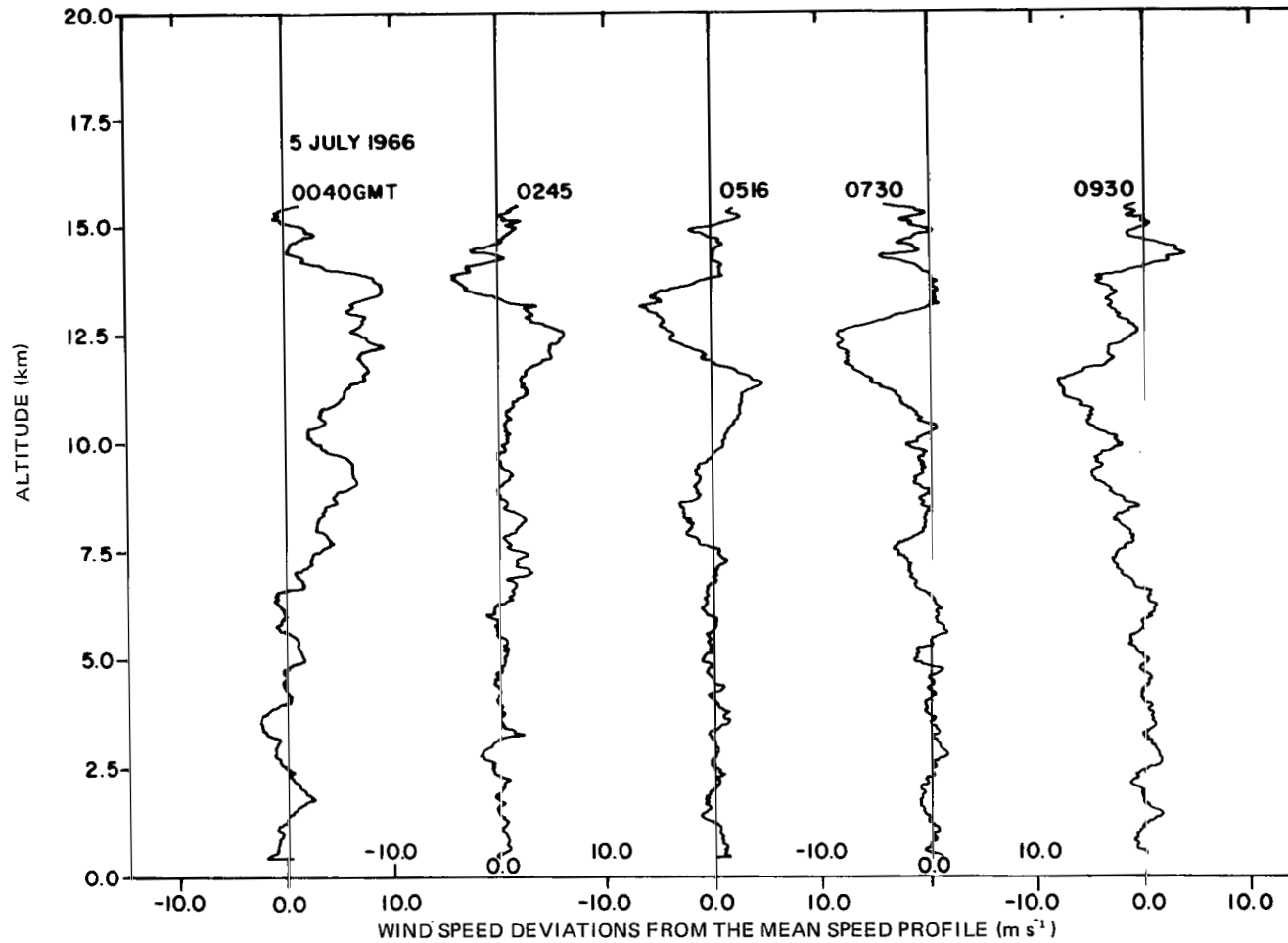
Figure 14.   Deviations of individual wind speed profiles from the mean profile,
July 5, 1966.
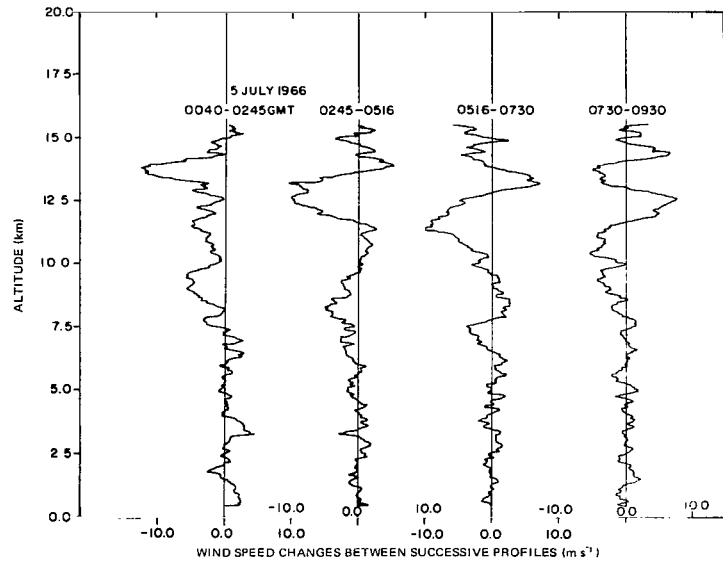
Figure 15. Speed changes between successive vertical
profiles, July 4-5, 1966.
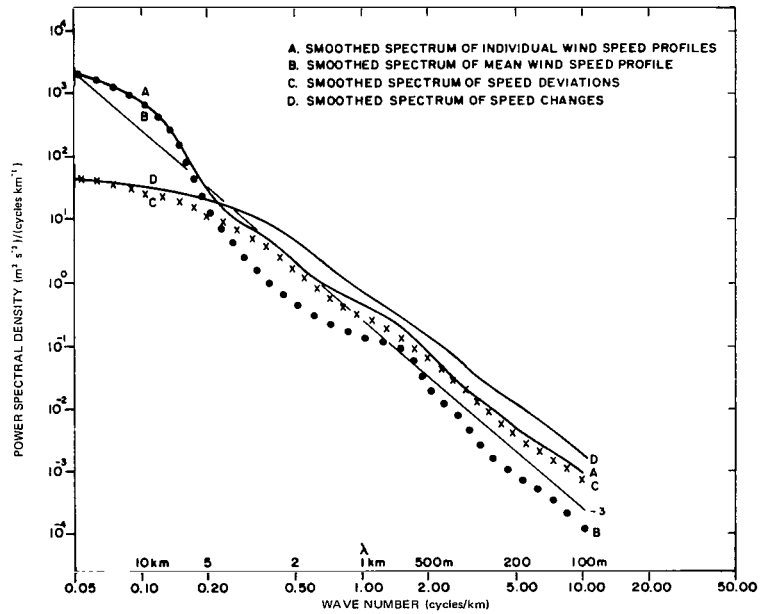
Figure 16. Summary of spectra of wind profiles,
July 4-5, 1966.

3. November Sequence of Wind Speed Profiles. On November 10, 1965, Cape Kennedy was under the influence of a flat surface pressure gradient with no active weather system over Florida, and winds aloft were of moderate speeds from the west. Four detailed wind profiles were measured between 1515 and 2130 GMT. Other profiles, measured at 1745 and 2245 GMT, terminated prematurely in the troposphere and are therefore not included in the discussion that follows.

The shapes of the four speed profiles designated a to d in Figure 17 are quite complex, particularly in the upper portions. This is also true of the average profile (curve e in Fig. 17). The spectra of these individual profiles generally conformed to a -3 line. The spectrum of the mean profile fell below a -3 line at high wave numbers as in the April and July cases. Evidently the jagged nature of the profiles in Figure 17 does not imply any preferred meso-scale structure, because the spectra did not have pronounced maxima or minima.
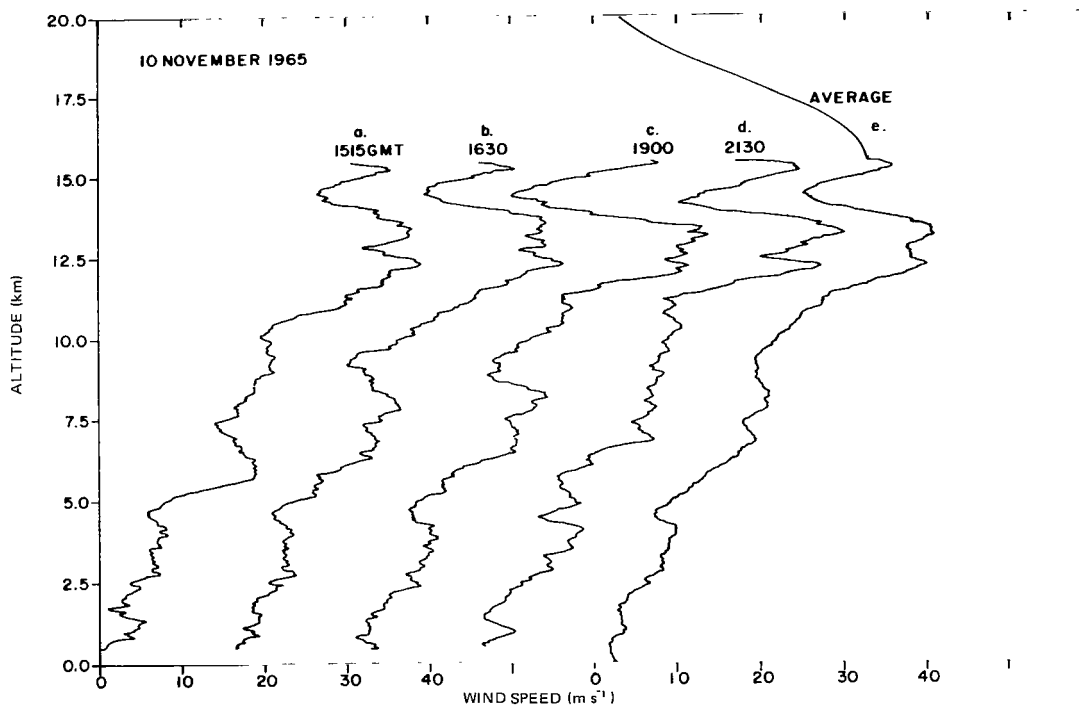
Figure 17. Sequential wind speed profiles measured at Cape Kennedy, November 10, 1965.

The deviations of individual speed profiles from the mean are shown in Figure 18. These deviation profiles are similar in appearance to those of Figures 10 and 14. For the most part, resemblances between successive deviations are not very great. The spectra of the individual speed profile deviations from the mean had nearly the same general shape as those of the April series.
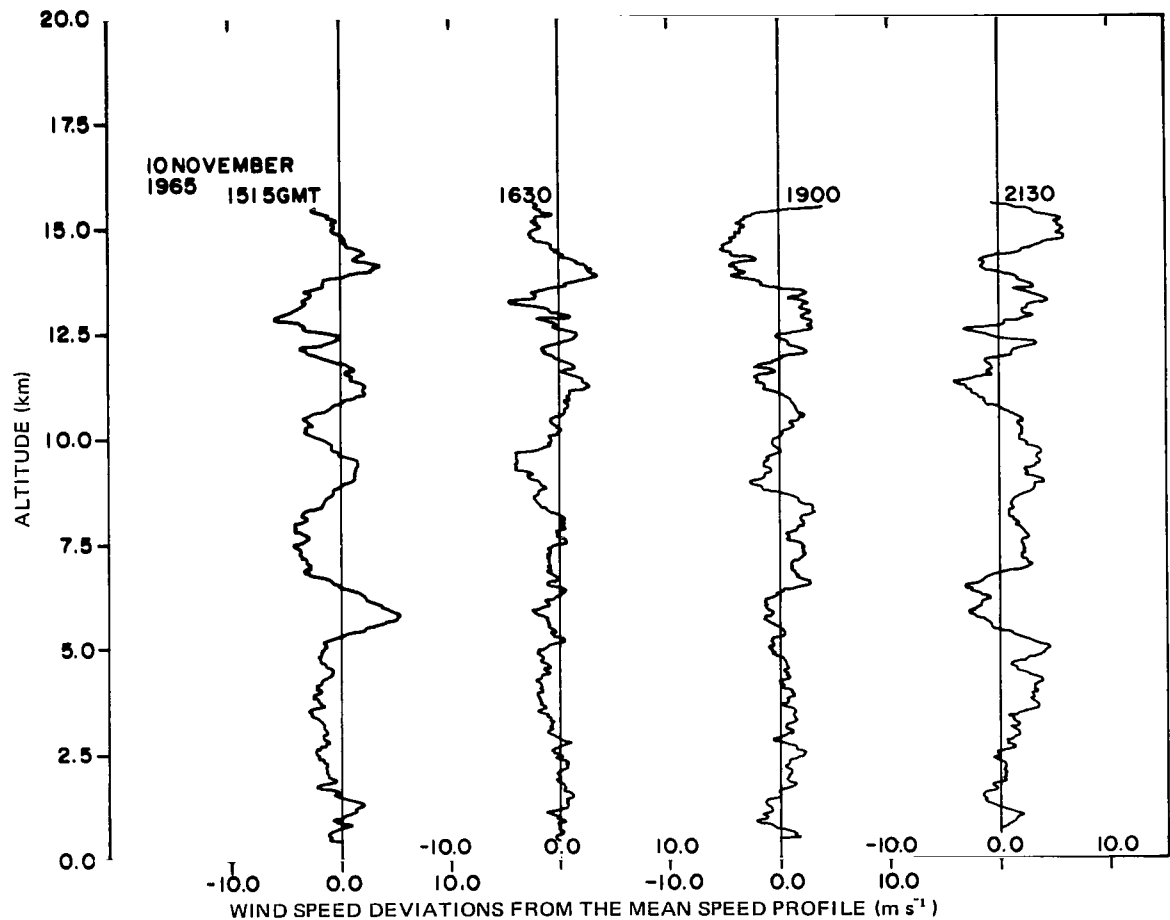
Figure 18. Deviations of individual wind speed profiles from the mean profile, November 10, 1965.

The changes in speed between successive profiles are shown in Figure 19. For the first change profile, the time interval is 1 h, 15 min, and for the latter two profiles it is twice as long. Changes are smallest below an altitude
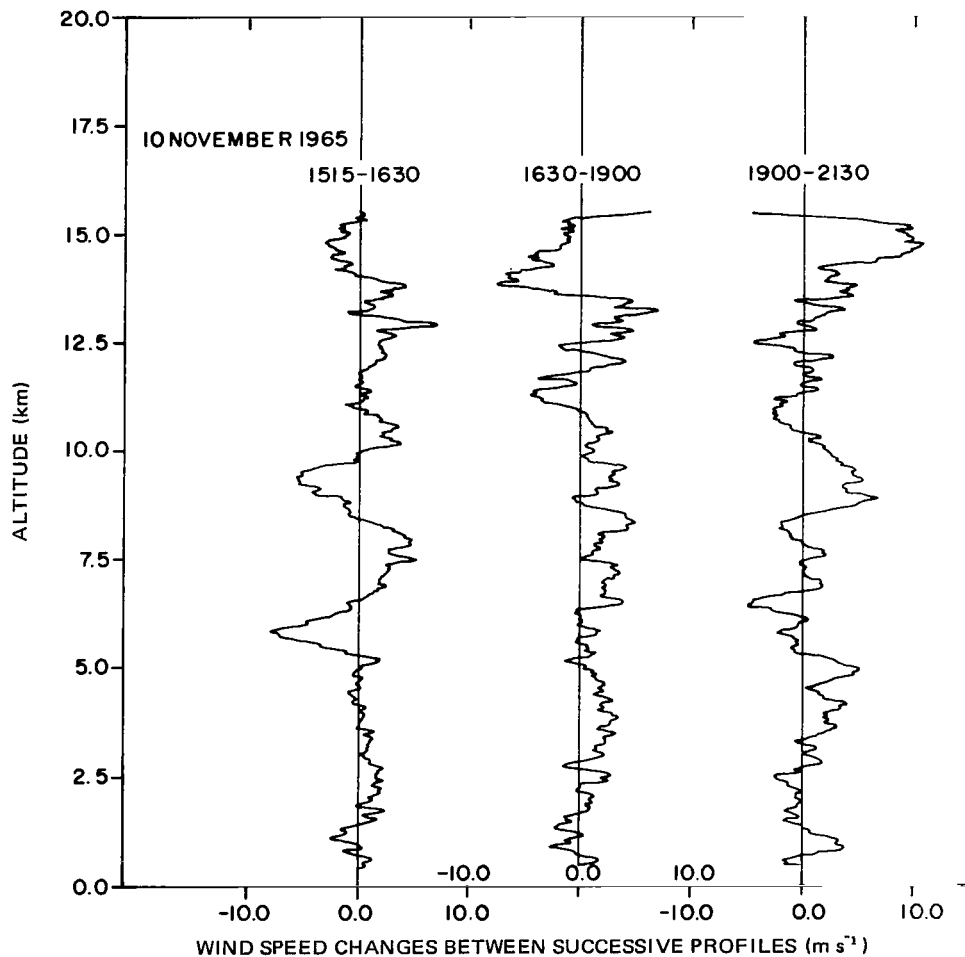
Figure 19. Speed changes between successive vertical
profiles, November 10, 1965.

of 5 km. It is difficult to discern any particularly consistent features in these
change profiles. Their individual spectra had similar features to the April
case except for a peak at a wave number of approximately 0.4 cycle km^{-1}; the
other two spectra cases for April and July flatten at approximately this point.

The spectra for this sequence are summarized in Figure 20 in a manner
analogous to Figures 12 and 16. The crossing points between curves A and D,
and also between B and C, are at a wavelength of approximately 1 km. Curve
D_1 refers to approximate 1 h time differences, and curve D_2 refers to approximate 2 h time differences. The smoothed spectra are the same except for wave
numbers less than 0.4 cycle km^{-1}, where curve D_2 has greater variances.
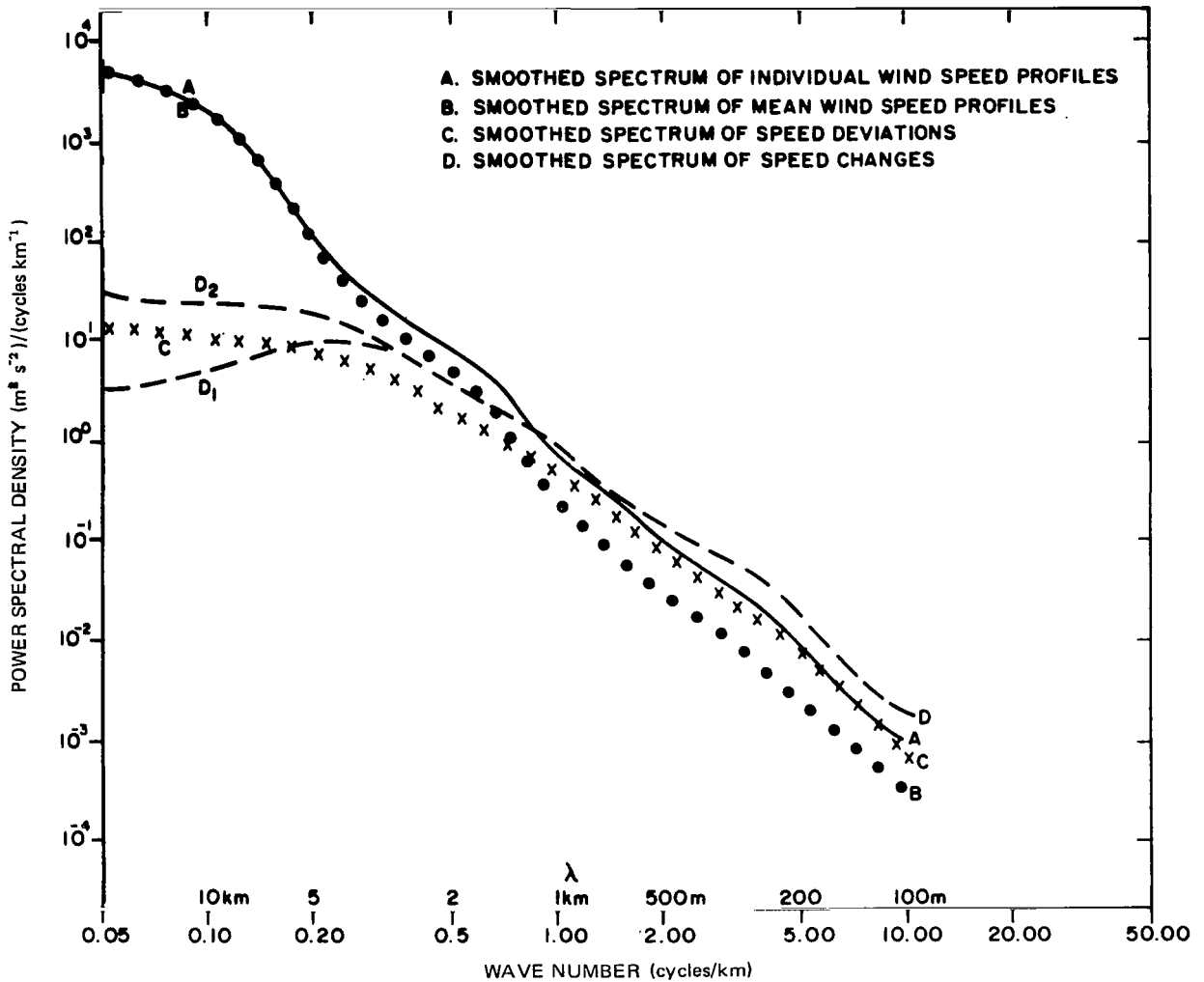
Figure 20. Summary of spectra of wind speed profiles,
November 10, 1965.

D. Discussion of Analysis

The properties of the smoothed average spectra for the three different
cases, encompassing strong winds of April 8, 1966, weak winds on July 5, 1966,
and moderate winds on November 10, 1965, are summarized in Figures 21
through 24. In Figure 21, the three smoothed spectra of individual profiles have
generally similar shapes. The major difference among the spectra is that the

33
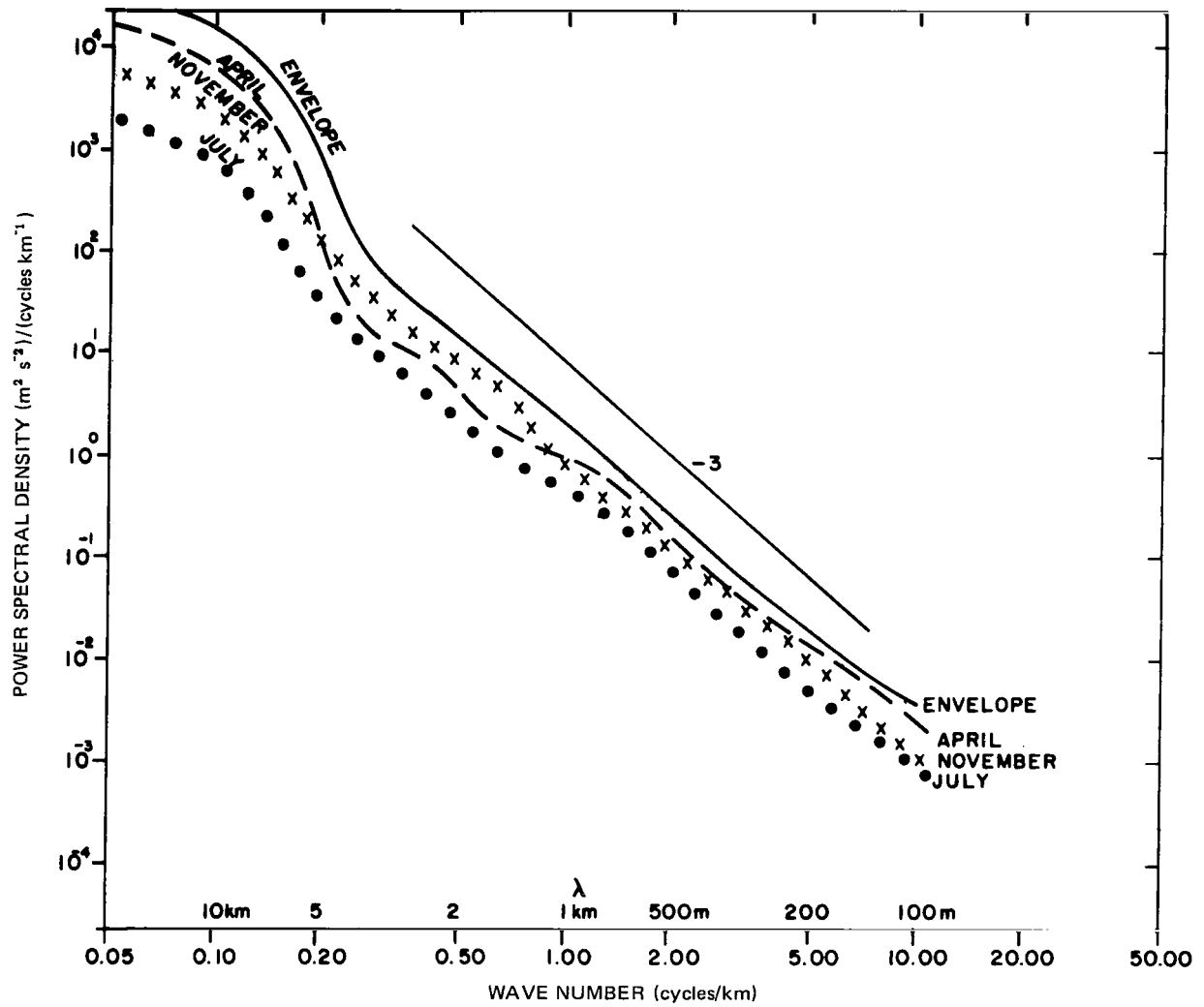
Figure 21. Smoothed spectra for the individual
wind speed profiles.
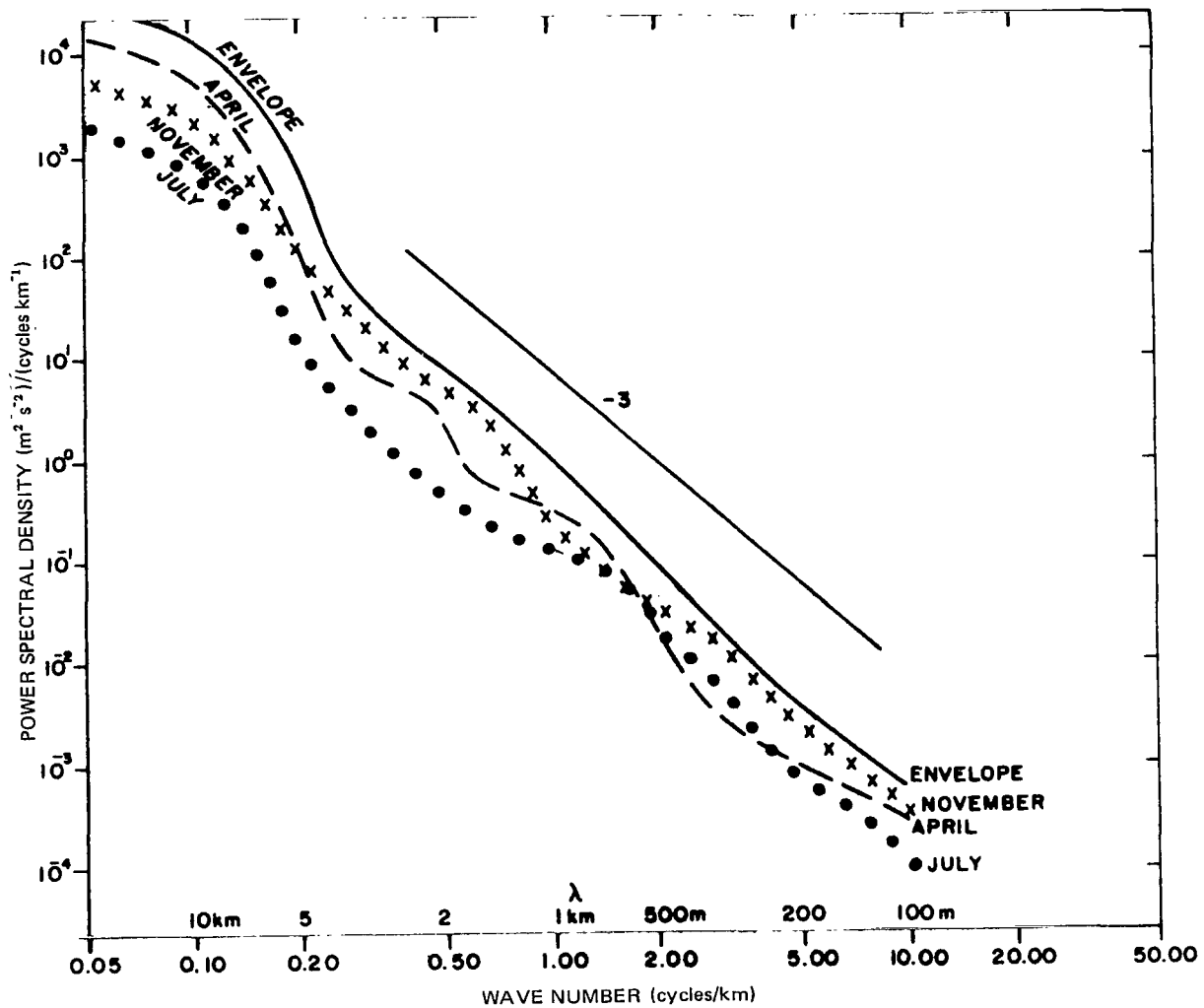
Figure 22. Smoothed spectra of mean wind speed profiles.
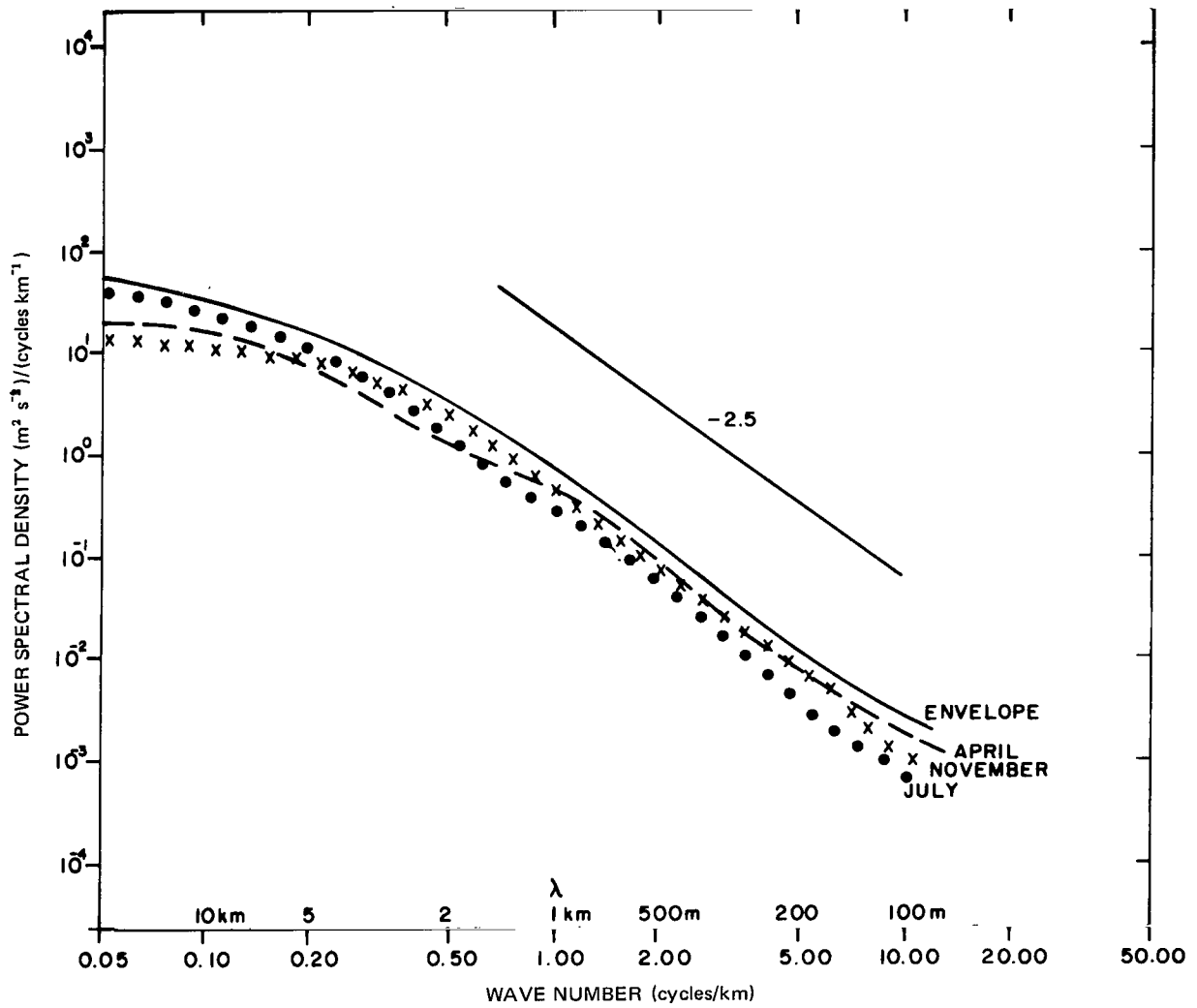
Figure 23. Smoothed spectra of deviation from mean profiles.
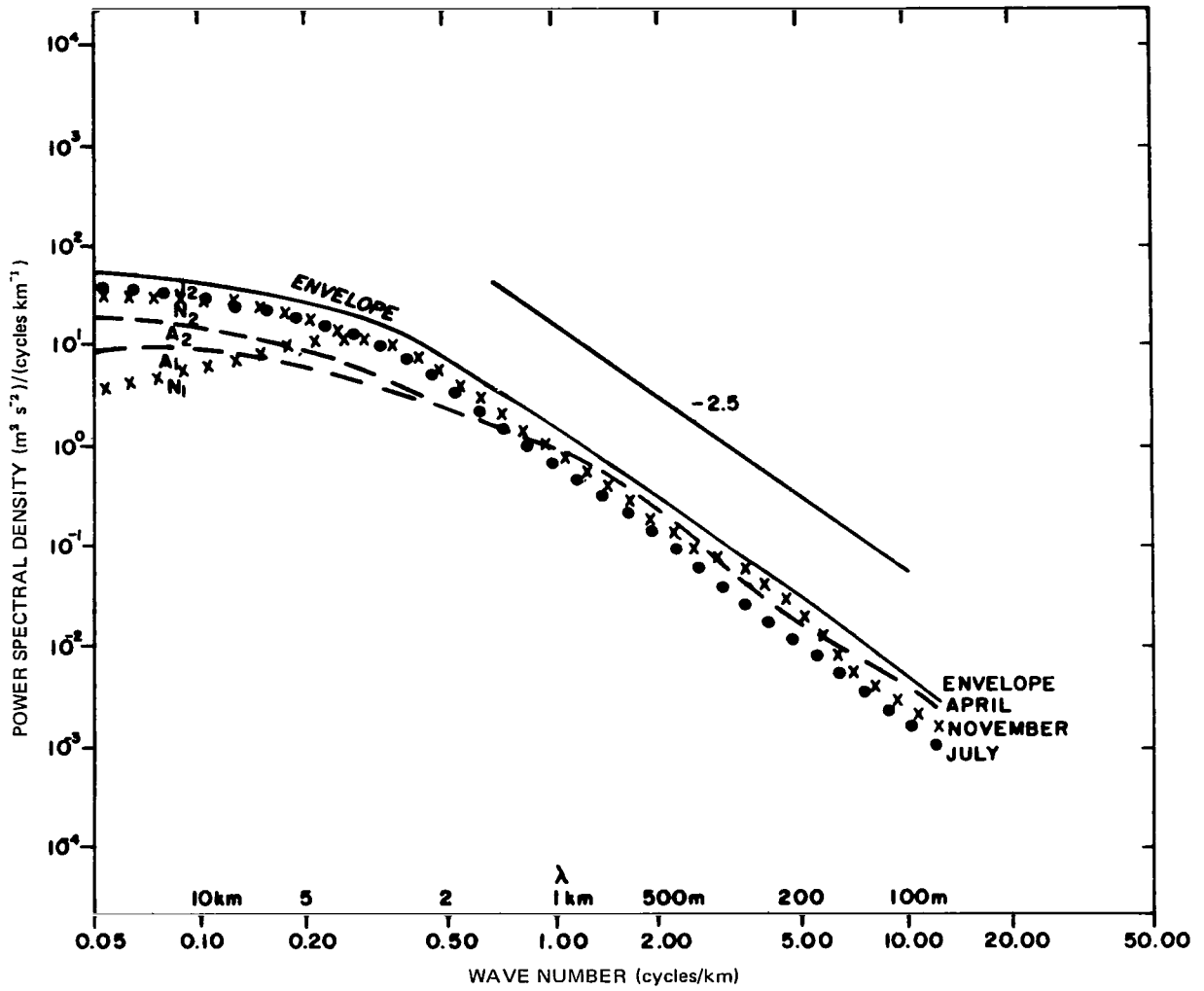
Figure 24. Smoothed spectra of speed change profiles.

power is greater at low wave numbers in proportion to the average wind speed of the profile. The minor relative gap in the April spectrum between frequencies of 0.2 and 1.0 cycle km^{-1} may be typical of strong winds but does not appear in the other two cases. In this portion of the spectrum, the jagged profiles of November 10, 1965, have the greatest energy. There are apparently no predominant scales to the speed variations along the vertical, and thus certain terminology, such as mesoscale in reference to vertical variations of 1 to 3 km extent, should not be understood to imply that this scale is a preferred or typical one. Instead, all scales are mixed together with rapidly decreasing energy as wave number increases. A curve which bounds the scatter of the individual smooth spectra of the three smoothed spectrum curves is also shown and is labeled envelope; smoothed spectra for most meteorological situations would probably lie below it.

The smoothed spectra of the mean wind speed profiles for April, July, and November are shown together in Figure 22. The -3 line is placed in the same position as in Figure 21 as a cross reference. As noted earlier, this represents the spectral slope one would predict for a buoyancy subrange. The curves of Figure 22 are similar to those of Figure 21, but have less energy at wave numbers above approximately 0.3 cycle km^{-1}. An approximate scatter band curve (envelope) is also shown.

The smoothed spectra of the deviations from ensemble average profiles for the three cases are shown together in Figure 23. They are remarkably similar at wave numbers above approximately 0.2 cycle km^{-1}. At the low wave number end, it is somewhat surprising that the case of weakest winds (July) has the largest energy. However, for these cases it may be explained by the lack of variability of low wave number content in the November and April profiles relative to the July profiles. The individual curves indicate a tendency for increasing power at low wave numbers with increasing time interval from the time of the mean profile. A scatter band curve (envelope) for the three cases is also given.

The smoothed spectra of speed changes between successive profiles are plotted in Figure 24. They are very similar at wave numbers above approximately 0.5 cycle km^{-1}. At low wave numbers, the July case has the greatest power (Fig. 23). The curves are also labeled with a 1 or 2 to denote whether the time change is approximately over 1 to 2 h. Those labeled 2 clearly have greater variance at low wave numbers. If the time interval were longer than 2 h, probably the left end of the spectra would gradually rise.

A scatter band curve (envelope) for changes over intervals of 2 h or less is shown. It lies somewhat above the scatter band curve of deviation (Fig. 23) at all wave numbers higher than approximately 0.1 cycle km^{-1}. To summarize Figures 21 through 24, the general characteristics of each type of spectrum (for measured wind speed profiles, deviations, and changes) are apparently not very dependent on season or synoptic situation.

Since the profile sequences discussed were selected without preconceptions, it is reasonable to expect that their characteristics are typical. An important result of the analysis is that the spectra do not show any preferred wave numbers that correspond to the macroscale, mesoscale, or microscale terminology. Apparently there are no clear-cut, natural separations between different scales of motion relative to vertical profiles. Instead, as far as spectrum shape is concerned, divisions between scales may be selected on an arbitrary basis.

E. Vertical and Horizontal Wavelength Relations

As mentioned in the Introduction, it is interesting to compare the spectra of vertical wind speed profiles to spectra of winds measured by aircraft flying horizontally across jet streams. In the latter case, the horizontal profiles in a south to north direction perpendicular to a westerly jet are similar in shape to the vertical profiles of Figure 9 except that the total horizontal distance is in the range from 500 to 1000 km. Kao and Woods (1964) have computed spectra from Project Jet Stream flights across strong jet streams (the average speed of the profiles was 63 m s^{-1}). Their spectra are for mesoscale deviations from a smoothed horizontal profile. A comparison of their spectra and those of Figure 21 shows that there is approximately the same power spectral density at a horizontal wavelength of 100 km and a vertical wavelength of 5 km. Similarly, power is approximately equal at 40 km and 2.5 km horizontal and vertical wavelengths. The range of mesoscale wavelengths having this property of approximately equal power is shown in Figure 25. Differences between the two computational methods may affect the diagram somewhat, but it is believed to be approximately correct. This comparison may have some application in selecting vertical and horizontal eddy exchange coefficients in detailed numerical prediction models.
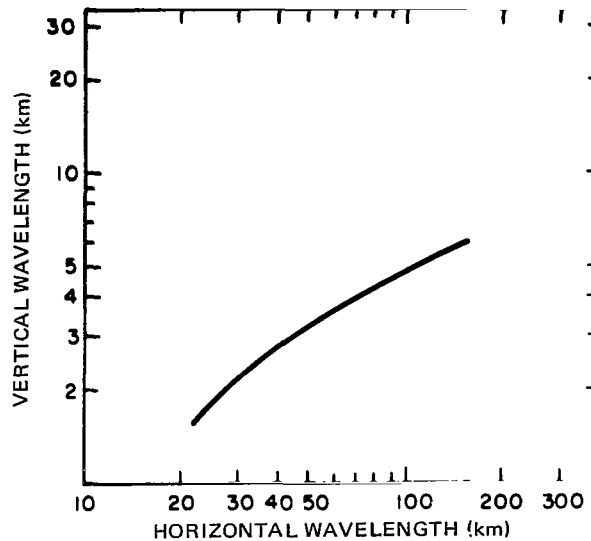
Figure 25. Comparison of vertical and horizontal
eddy scales that have same power spectral density
in the mesoscale region.

It is noted that for cases of moderate or greater clear air turbulence,
Pinus (1963) shows that the power in horizontal mesoscale wind variations is
more than an order of magnitude larger than that given by Kao and Woods
(which were for cases of predominantly smooth flight). It seems doubtful
that the high energy levels of clear air turbulence can be attributed to transfer
of energy from relatively long vertical or horizontal waves that have greater
power. Therefore, the present analysis is consistent with the concept that the
energy input to clear air turbulence probably arises from unstable shear-gravity
waves (produced either by internal flow patterns or obstacles such as moun-
tains) and the interaction with shear (Bekofske, 1972) and not from macroscale
variations in the wind field.

IV. MODELS AND PHYSICAL MECHANISMS

A. Model Assessments

Three possible physical models of mesoscale circulation to explain the
observed shears were selected for study: (1) paired longitudinal vortices
(helicance), (2) phase shifts with height of standing gravity waves (buoyancy

40

waves) in successive atmospheric layers, and (3) stacked layers of alternating inertial oscillations. Each model is supported by some segments of the data and contradicted by others. Actually, all mechanisms are operating; the smallest scales are probably gravity waves with occasional layers of turbulence in the true sense of the word. As the vertical scale increases, Coriolis forces will become important and gravity-inertial waves will exist. The larger scales are probably characterized by inertial modes. Another aspect of the motions one sees on the detailed wind profiles is that in the troposphere they may be convective in origin while the perturbations in the stratosphere have gravity wave or gravity-inertial wave origins. This assessment utilizes information developed by Weinstein and Reiter (1965).

The model which appears most suitable pictures the wind regime as the result of the horizontal motion of stacked layers of large horizontal extent. The layers have sufficient stability to operate relatively independently. Motion within each layer appears to be controlled principally by a quasi-inertial oscillation around the basic geostrophic flow at that level. The vertical shears arise in part because the inertial oscillation amplitude and phase of one layer are not correlated to the amplitude and phase at other layers. The shear magnitudes slowly evolve as the phases evolve. The maximum possible shears are limited by the local stability through a Richardson's number criterion (Vinnichenko et al., 1973).

1. Paired Longitudinal Vortices (Helicance). The first model postulates stacked layers of oppositely directed or paired longitudinal vortices. In a report on a very comprehensive series of laboratory experiments, Avsec (1939) described three principal types of thermoconvective eddies: (1) Benard cells, (2) "eddies in transverse bands," and (3) "eddies in longitudinal bands." Benard cells are well known; the only point added here is that under the right conditions of vertical shear these cells align themselves into a wormlike chain. The rare eddies in transverse bands were aligned perpendicular to the mean flow and evolved from wave crests and troughs. The final type of eddy was similar to that described by Helmholz et al. in conjunction with banded cirrus clouds. Coexistence of two or more of these eddies and transformation from one type to another was common. Avsec credits Idrac (Benard, 1936) for the thought that the conditions realized in the high atmospheric layers of the troposphere were favorable to the formation of regular eddies like those obtained in the laboratory. Idrac had discovered periodicity of ascending and descending currents in the low atmospheric layer in direct contact with flat ground. Idrac

41

had also observed the planning flight of large birds grouped in parallel bands approximately 200 or 300 m apart. Recording apparatus showed that these birds were placing themselves regularly above the rising airflows that were aligned in the general direction of the wind. Idrac supposed that the layer of air sweeping the heated soil became, by reason of the vertical instability, the seat of convective movements in the shape of gigantic rolls. Winds above the ocean were found to have a similar structure but with smaller ascending speeds.

Kuettner (1959), when discussing banded structure (cloud streets) of cloud systems, described a flow similar to what is called helicance here. He described cloud streets as oriented in the general direction of the flow. This longitudinal banded structure covers a considerable portion of cloud layers and may be found at all latitudes. Kuettner cited the experience of glider pilots who use the term "wind thermal" to express their observations that a combination of thermal convection and strong winds is required to produce cloud streets. He described typical dimensions for cloud streets to be 50 km in length and 5 to 10 km in spacing from axis to axis. However, he further states that cloud streets of several hundred kilometers have been observed with characteristic layer depths of 1.5 to 3 km, where the crosswind spacing of the cloud street lies frequently between two and three times the height of the convection layer. He described cloud streets as having a lifetime of the order of 1 h. They appear to build up and dissipate on both ends, sometimes in a fashion that suggests that the street as a whole drifts slower than the wind. The dissipation is often seen to start through interference with other growing cloud streets. Glider observations show that vigorous updrafts exist under certain sections of the cloud base, while downdrafts essentially occupy the space between the cloud bands. Under otherwise similar conditions, the updrafts below cloud streets are generally estimated to be stronger than the flow in columnar thermals.

Conover (1960) described similar cirrus bands tending to be parallel to the jet stream on the warm side and near the entrance (upstream from maximum wind speed core of the jet stream principal axis). He observed three categories of longitudinal bands according to the average spacing between bands. The "major bands" were spaced 4.2 km apart and were 148 km long. The following is quoted from the abstract of his paper:

> The major bands are created between parallel horizontal vortices through which the air flows in a helical motion. The vortices rotate in opposite directions and cloud forms where the combined motions is upward. The resulting clouds indicate conditional instability in all cases, and their form apparently depends on the steepness of the lapse rate and prevailing

vertical shear. Maximum lateral components of motion measured across the tops of the vortices range from 0.6 to 6.0 m sec^{-1}. When these components are combined with the forward speeds, a median angle of 4.4 deg from the large-scale wind direction is found across the tops of the vortices.

If two vortices are assumed for each major band interval, the average vortex width would be 2.1 km. It was observed that the ratio of band spacing to depth of the overturned layer was 1.6, which gives an average horizontal-vertical vortex dimension ratio of 0.8. There have also been other reported observations of similar banded-type clouds and associated vortex-type circulations (Clem, 1954, and Schaefer, 1957).

Woodcock (1942) from observation of soaring birds, Pack (1962) from the motion of two tetroons, Smith and Wolf (1963) from ground dosage of tracers, and Mee (1964) from aircraft observations of temperature and mixing ratio have found evidence for helicance-type circulations in the boundary layer near the Earth's surface over smooth ground or water surfaces. The general characteristics of the atmospheric vortices as indicated by the investigators are:

a. The ratio of horizontal (normal to axis of helicance) to vertical dimensions is of the order of unity.

b. The lateral components of air motion are small (Conover found 0.6 to 6 m/s).

The helicance model has its appeal because it explains the observed oscillation in the Jimsphere balloon rate-of-rise (DeMandel and Krivo, 1971) much more effectively than do the other two. It would explain the oscillations in scalar wind speed with height and their persistence; however, it would be totally unable to allow for the similar persistence in the wind direction oscillations. The only way the latter could be explained is by postulating that these helicances move across the station at precisely the correct speed to allow successive Jimsphere balloons to rise into alternate helicances. This appears highly unlikely. Also, there have been no published accounts of stacked paired vortices. Brunt (1939) stated that vertical stacking of vortices is theoretically possible but would be a highly transitory phenomenon.

A simple experiment was conducted to investigate the possible dimensions of the horizontal and vertical perturbations in the mesoscale structure. Two Jimsphere balloon tracks (1951 Z and 0224 Z) approximately 14 h apart are plotted in Figure 26. The inset in the lower left shows the separation rates of successive balloons. It can be seen that the same perturbation in the wind profiles (Fig. 27) was observed over a considerable horizontal area (approximately 20 km in the case of the perturbation at the 17 km level). The horizontal to vertical dimensions ratio of paired vortices which could be responsible for such wind fluctuations would have to be an order of magnitude larger than the theoretical value derived by Avsec (1939) and anywhere from 2 to 10 times larger than the maximum values observed by the other authors.

Another apparent problem with the longitudinal vortex theory relates to the three dimensional vortex motion. The circulation must include substantial vertical air motions between the horizontal boundaries. This vertical motion, taking place adiabatically, would require a temperature sounding close to neutral within the vortex layer. The available temperature profiles, although crude, have sufficient accuracy and vertical resolution to show that such near-neutral regions are not associated with the velocity oscillations in many cases.

A further major drawback to this model is the observed persistence of the wind fluctuations. It is difficult to conceive of such shallow and, hence, narrow vortices remaining in an exact orientation relative to successive ascending Jimsphere balloons for many hours (particularly as successive balloons sometimes cover different geographic paths, as shown in Fig. 26).

Since it has been clearly shown that paired longitudinal vortices exist in the atmosphere, they must be contained in the small transient wind perturbations observed in the detailed wind profiles. They do not, however, appear to be the cause of the persistent mesoscale perturbations.

2. Buoyancy or Internal Gravity Waves. The second model is frequently employed to explain perturbations in wind profiles similar to those observed in the present investigation. This model explains the perturbations as manifestations of buoyancy or internal gravity waves. The horizontal velocity variations are deemed to be the result of a thickening or thinning of the layer containing them as the air moves through buoyancy waves which are not in phase in the vertical. Buoyancy waves appear to always be present to some degree when a region of significant stability exists in the troposphere (Gossard, Richter, and Atlas, 1970). Hines (1960) gives a thorough description and theoretical treatment of this phenomenon. He showed that it could be responsible for observed
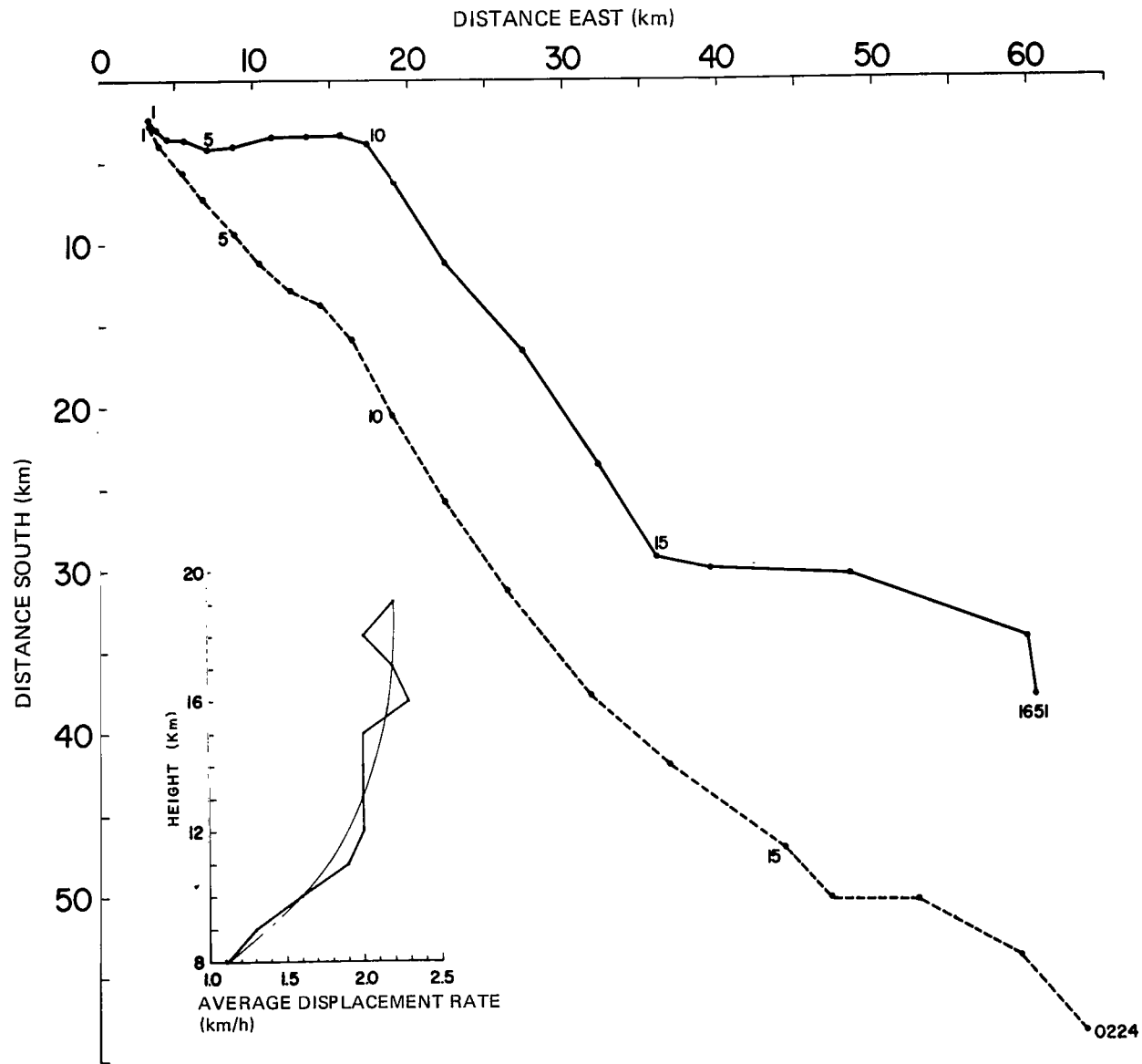
44

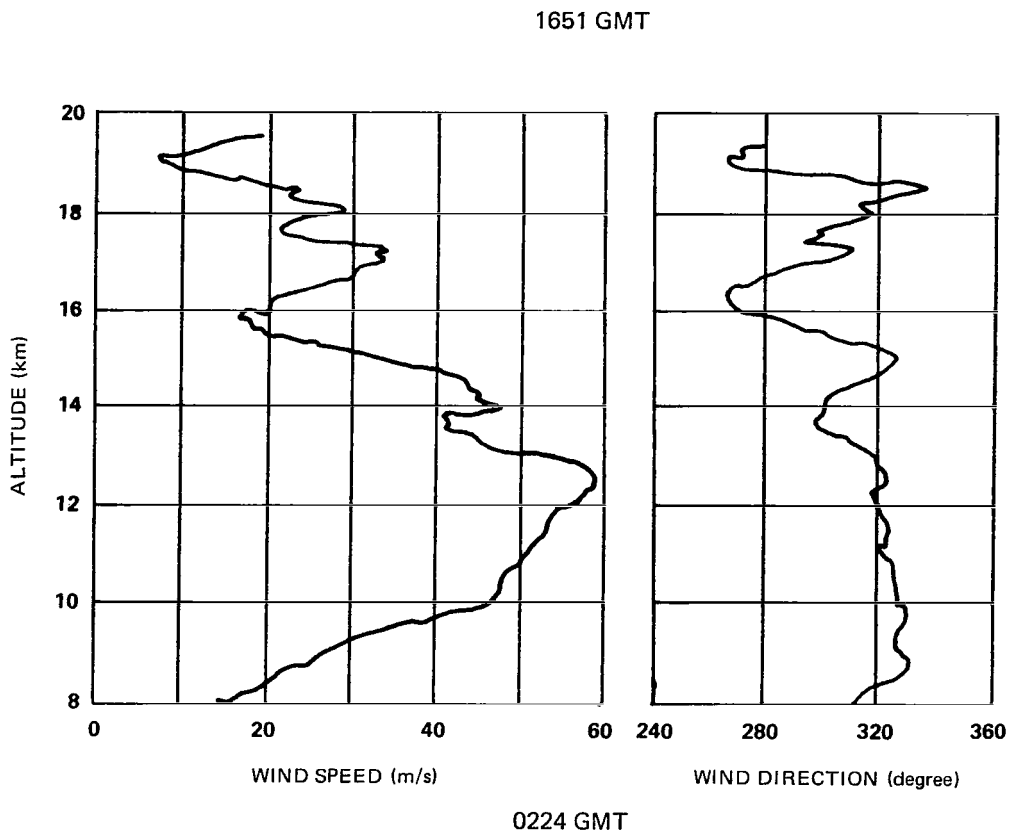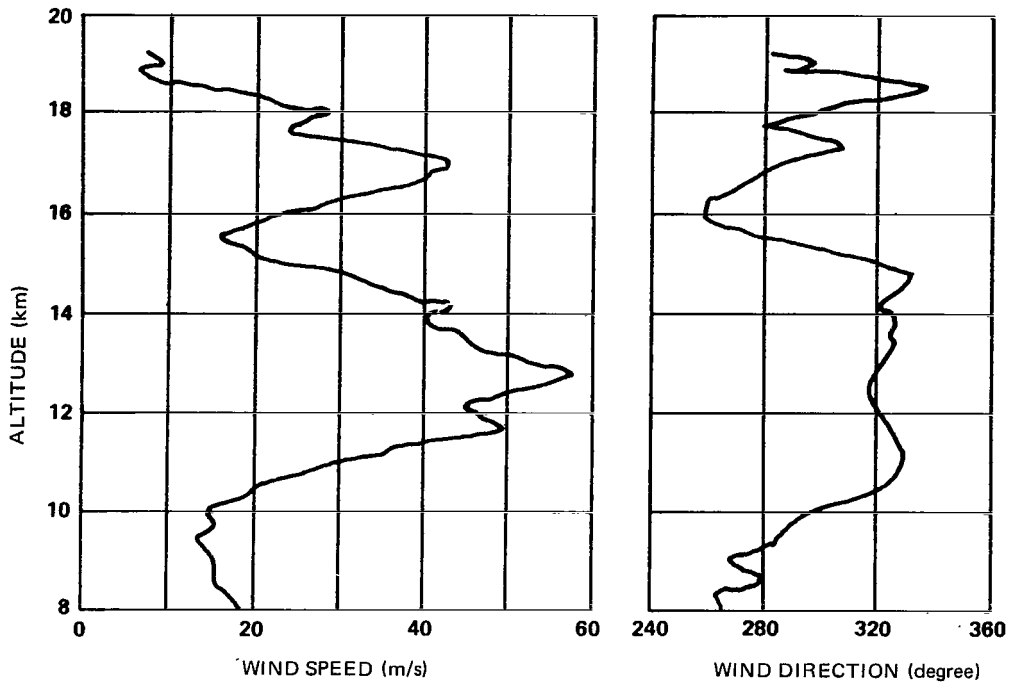Figure 26. Two Jimsphere balloon tracks (altitude identification in kilometers shown on solid curve).

Figure 27. Two wind speed and direction profiles (associated
with Fig. 26, Jimsphere balloon tracks).

wind speed features in the stratosphere with vertical wavelengths of 12 km. When his equations are applied to measured vertical oscillations in the altitude range from 11 to 20 km, it is found that the vertical wavelengths of the wind oscillations with a period of 10 h should be two orders of magnitude less than the horizontal wavelengths of the buoyancy waves. In the present context, standing buoyancy waves (lee waves) must be investigated first as a perturbation source because they offer the best explanation of the persistence of the wind fluctuations. It could be postulated that the standing waves are generated by the thermal and frictional differences between land and sea along the coasts of California (Point Mugu data) and Florida (Cape Kennedy data). Lee wave theory, however, states that the horizontal and vertical wavelengths should be of the same order of magnitude (Scorer, 1949). To make this statement consistent with the calculation previously mentioned (i. e., to say that the wind features from 11 to 20 km altitude, where the horizontal wavelength exceeds the vertical by two orders of magnitude, are manifestations of standing waves near the surface of the Earth where lee wave theory states the wavelengths should be the same order of magnitude), it must be postulated that the horizontal wavelengths increased by 200 times within less than 20 km height. At present there is no indication of such a wavelength increase.

In an effort to determine the order of magnitude of the horizontal wavelength of a lee wave which could be produced with the wind speed and direction profiles shown in Figure 27, the maximum horizontal wavelength according to lee wave theory was calculated. This wave length is given by equation (1), where g is gravity, θ is potential temperature, Z is altitude, and V is speed of wind:

$$\lambda = 2\pi \frac{V^2}{\frac{g}{\theta} \frac{\partial \theta}{\partial Z}} \quad . \tag{1}$$

The result is a maximum horizontal wavelength of 45 km. In contrast, Hines' (1960) theoretical studies called for a gravity wave to have a horizontal wavelength or approximately three times this value to produce the mesoscale perturbation observed in the vertical profile at 17 km altitude, as noted in Figure 27. With a vertical wavelength of approximately 3 km, the lee wave horizontal wavelength should be of an order of magnitude, or 30 km, and the buoyancy wave horizontal wavelength should be of two orders of magnitude, or

300 km. To resolve this issue, additional data in the form of detailed vertical wind and temperature profiles are required from a network having sufficient spatial resolution to resolve the horizontal and vertical wavelengths.

Free buoyancy or internal gravity waves may be a source of the persistent mesoscale wind fluctuations over periods of 8 to 10 h, such as those described herein, only if the ratio of horizontal to vertical wavelengths is of the order of 100:1. In this case they propagate very slowly and behave almost like a stationary phenomenon. These waves, however, would produce wind speed perturbations an order of magnitude smaller than those observed in the present data. To produce the mesoscale wind speed perturbations of the observed order of magnitude, a period of approximately 1 to 2 h is required. This does not conform to the persistence of perturbations over at least 6 h, as is evident from the data presented in Appendix B.

The internal gravity wave model only allows for very persistent wind features (both maximums and minimums) as long as one may assume a steady state of the atmosphere. In such a case, there would be reason to expect that the balloon would go through the same parts of the system during each ascent. A major limitation on the model is the rather deficient schemes used to describe the mechanisms favorable or unfavorable for lee wave generation. It is difficult to explain a series of mesoscale oscillations by a model involving lee waves when it is not even known if a lee wave could exist at the time of the balloon ascents. Gossard and Hooke (1975), after considerable analysis and review of literature, concluded that the mechanisms have yet to be confirmed experimentally, or remain poorly understood. This is especially true for the troposphere and its complex interactions of buoyancy and other waves due to convective activity, orographic features, frontal systems, shear instability, etc.

To provide a satisfactory explanation, the internal gravity wave or buoyancy model would also require phase differences in standing gravity-type waves (lee waves) contained within stacked layers. This would require the crest of the wave in the lower layer to be aligned with the trough of the wave in the upper layer, in which case one would expect a wind speed maximum. Where the trough of the lower wave is aligned with the crest of the upper one, a wind speed minimum would be expected. If several of these crest trough systems were stacked one above the other, as is often observed in lee waves, the measured mesoscale speed oscillations might be explained.

48

3. Quasi-Inertial Oscillations. The third model calls for stacked layers of air undergoing quasi-inertial oscillations. These layers are relatively thin and stable and — unless turbulent forces or convective motions are present — could maintain themselves for considerable periods of time and over wide areas.

Sawyer (1961) has described quasi-periodic wind variations with height in the lower stratosphere, persisting for periods of hours, based on observations made at Crawley, England. The Crawley oscillations were similar in characteristics to those observed by the Jimsphere radar system. Sawyer described the disturbances which give rise to these variations as having vertical dimensions of approximately 1 km and horizontal dimensions much greater (at least several hundred kilometers). He further used perturbation theory to show that slow inertial oscillations might have such dimensions. He concluded that these disturbances in the stratospheric wind flow were the result of a balance between inertial, Coriolis, and static stability effects.

Barbé (1958), using an automatic-following radar, found oscillations similar in amplitude to those described by Sawyer. He found that these wind variations occur over layers 1 or 2 km thick and that their main features, including the altitude of maximum and minimum wind, were repeated on soundings separated in time by periods of 5 to 10 min. Clem (1954), using rawinsonde observations, reported similar fluctuations with height, but these fluctuations were considerably greater in amplitude than those found at Crawley. Reiter (1958) suggested that the rawinsonde oscillations might be of instrumental origin because their wavelengths coincided with the periods of observation and smoothing. Neiburger and Angell (1956) observed inertial oscillations in the tracks of constant pressure balloons. The rather small vertical movements of these balloons probably allowed them to sample oscillations within a rather narrow altitude layer.

Reed, Azim, and von Gohren (1964) used Sawyer's results, rocket trails, and ozone concentrations to support the existence of oscillations in the stratosphere. Danielsen (1959 and 1964) stressed the laminated structure of the atmosphere showing that small scale structure in lapse rate persists for considerable periods in time and space. Weinstein and Reiter (1965) found some of the wind oscillations to be associated with lapse rate discontinuities.

The quasi-inertial oscillation model has considerable appeal because the wind speed and direction in successive layers would not necessarily have to be in a strict and constant phase relationship. The only requirement would be

that the period of the oscillation along an isentropic surface should be close to or larger than one-half a pendulum day. The principal drawbacks to this model are:

a. The data seem to indicate that the periods of the oscillations along isentropic surfaces are less than one-half a pendulum day. This would require some shortening mechanism, as described by Sawyer (1961).

b. This model would not account for the observed oscillations in the Jimsphere balloon rate-of-rise profiles (data not shown in present study) because it does not contain large scale organized vertical motions. Such oscillations would require a mixed gravity-inertial wave mode to exist.

The word "quasi" is inserted for the model because the geostrophic basic flow about which oscillations occur may not necessarily remain constant in time. Furthermore, frictional forces and diabatic effects may have modifying influences. Even if the complicating factors were not present, a true inertial period of one-half a pendulum day (approximately 22 h at the geographical latitude of these wind observations) need not be observed in the single station series of Jimsphere balloon ascents, as inertial motions of air parcels are described in a Lagrangian coordinate system. Their behavior in an Eulerian system, in which the present data are described, depends upon the advective properties of the oscillations, about which only assumptions can be made.

In spite of the aforementioned limitations, the quasi-inertial oscillation model could easily account for two significant characteristics of the observations, namely the persistence and horizontal extent of the perturbations. While the quasi-inertial oscillation mechanism is probably not the only one operating on the persistent wind fluctuations, it appears to be the most important one. Newton (1959) studied ageostrophic inertial oscillations in connection with jet streams and concluded that the oscillation of particle wind speed in the jet core could be up to twice the inertial period, or one pendulum day. Quasi-inertial oscillations may be more common in the atmosphere than traditionally believed.

In evaluating the plausibility of the explanation of the shears as manifestations of inertial oscillations, one should consider whether geostropic wind variations in the vertical could be sufficiently strong to account for the observed shears. Taking an extreme horizontal temperature gradient such as that associated with jet stream conditions (e.g., 5°C/100 km) yields a vertical gradient of geostropic wind speed of approximately 0.02 s^{-1}, several times stronger

than the shears found here. However, the shears of this study often alternate in sign and, if generated solely by geostrophic wind, would require unreasonable vertical temperature gradients (some of the gradients being self-destroying because of instability). The dominant wind oscillations for the normal weather situations studied here must be ageostrophic.

B. Effects of Quasi-Inertial Oscillations on Wind Profiles

In this section it will be shown how quasi-inertial oscillations could produce a persistent mesostructure in the wind speed and direction profiles together with some of the characteristics these profiles would possess.

Consider the horizontal wind at a particular altitude level (V_T) to consist of a geostropic component (V_g) and an inertial component (V_i) (Fig. 28). The former is constant in magnitude and direction, while the latter is constant in magnitude but rotates anticyclonically with the period of the quasi-inertial oscillation. It can be seen that total wind at any instant depends upon the phase of the inertial cycle at that time.

Envision several such inertial cycles stacked vertically and superimposed upon a profile of basic geostropic flow which, for simplicity's sake, is assumed to have const. ut vertical shear above and below the level of maximum wind. In Figure 29, inuependent inertial oscillations similar to those in Figure 28 are assumed at levels 1 through 7. The geostropic component of the wind is shown by the dashed arrows and the total wind by the solid arrows. If each layer of
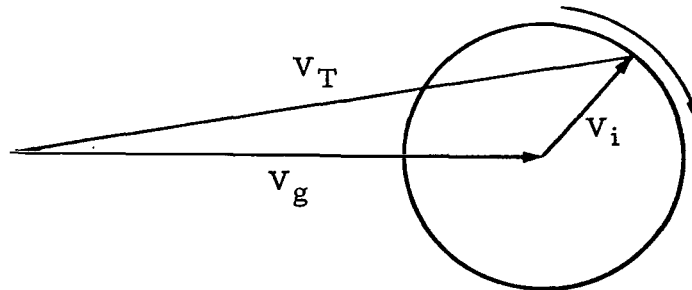

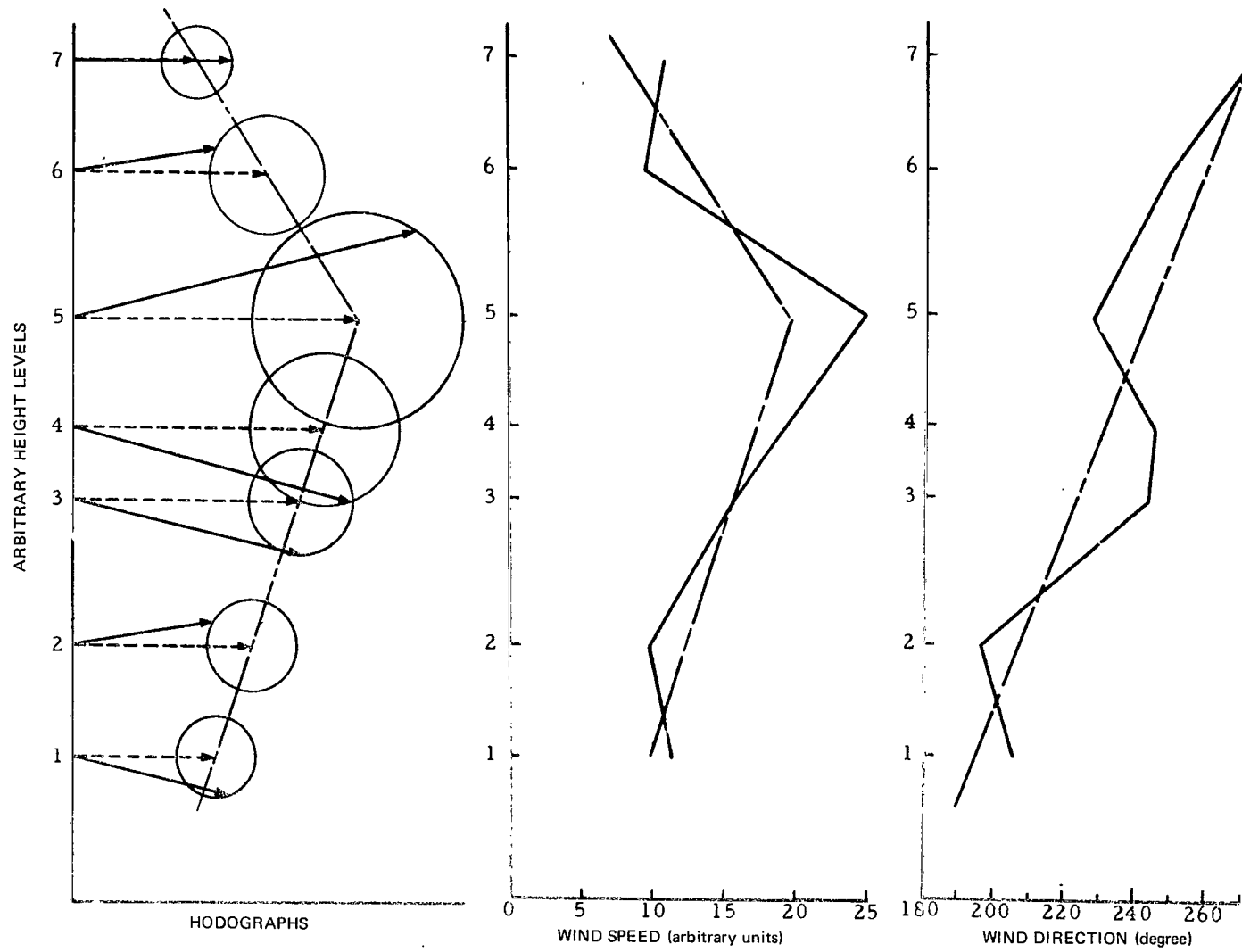Figure 28. Wind velocity variation through an inertial cycle (horizontal layer at a given altitude level).

Figure 29. Illustrative model of stacked quasi-inertial oscillations.

inertial motions were completely detached from its surroundings, vertical discontinuities in wind speed and direction would result. These could not be maintained under the influence of turbulent forces. Such forces would tend to generate finite shears between layers. In the schematic profiles of wind speed and direction (Fig. 29), linear shears were assumed to extend between the centers of each oscillating layer, in line with observational evidence (Appendix B). A vertically rising balloon, encountering oscillations at a different phase, thus would measure the wind profiles shown in the right-hand portion (solid line) of Figure 29.

The following characteristics of wind speed and direction profiles produced as described by this model should be noted:

1. No definite phase relationship between wind speed and direction perturbations is expected if the phase angles at which individual inertial oscillations are encountered remain undetermined.

2. For a true inertial oscillation, a maximum (minimum) deviation from geostrophic wind speed should correspond to a minimum (maximum) deviation from geostrophic wind direction.

3. The maximum vertical wind shears occur where two successive inertial oscillations are directly out of phase and the ageostrophic wind shear thus generated has the same signs as the basic geostropic shear. The total wind direction change with height in such a situation is simply given by the geostrophic wind direction profile.

4. Maximum changes of wind direction with height should be found when two successive inertial oscillations are directly out of phase, one-quarter of a cycle removed from the time of maximum wind shear. The vertical wind shear in this case is given by the geostrophic wind speed profile.

C. Evidence in Support of the Quasi-Inertial Oscillation Model

1. Temperature Soundings and Richardson Number. The existence of the horizontal inertial oscillations depends on the suppression of momentum exchange resulting from turbulent mixing in the layers in question. Thus, the

temperature soundings should show stability at appropriate layers. Actually, stability must be interpreted within the context of the Richardson number (Ri) rather than from temperature profiles:

$$Ri = \frac{\frac{g}{\theta} \frac{d\bar{\theta}}{dZ}}{\left(\frac{d\bar{V}}{dZ}\right)^2} \quad , \tag{2}$$

where, g is gravity, θ is potential temperature, Z is altitude, and V is wind velocity. The critical value of Ri differentiating between decaying and growing turbulence has not yet been accurately defined; values of 0.25 to 1.0 are in common use, although theoretical and experimental evidence suggests that instability could exist where Ri is less than 0.25 (Lloyd, Low, and Vincent, 1972). Therefore, in this research, Ri < 0.5 denotes turbulence, Ri > 1.0 means stability, and 0.5 < Ri < 1.0 is indeterminate.

The only temperature data available for the period of the Jimsphere radar wind soundings are from standard radiosonde runs and have much less vertical resolution than the corresponding wind data. In Figure 30 the temperature sounding is given together with the associated wind speed and direction profiles. The layers of temperature inversion are shown. There is no obvious correlation between these layers and significant points on the wind profiles.

Figure 30 also shows the profiles of Ri. The use of Ri computed from a single wind and temperature profile is valid in this case because it has been shown that the features are very consistent with time. Ri was computed over layers within which temperature lapse rate and wind shear were linear; the depth of the layers ranged from 100 to 1000 m. Here the correlation between details of stability and velocity is somewhat easier to interpret. There are three layers (at 12, 14, and 18 km altitude) where Ri is very large, and each one can be associated with a shallow region of a double reversal of wind speed. The large single velocity peaks at 13 and 17 km are in regions of low Ri between layers of high Ri. Stacked quasi-inertial oscillations, as described in Figure 29, may explain these features. Some turbulence evenly distributed through a layer undergoing an inertial oscillation should cause the velocity to peak in the center of the layer.
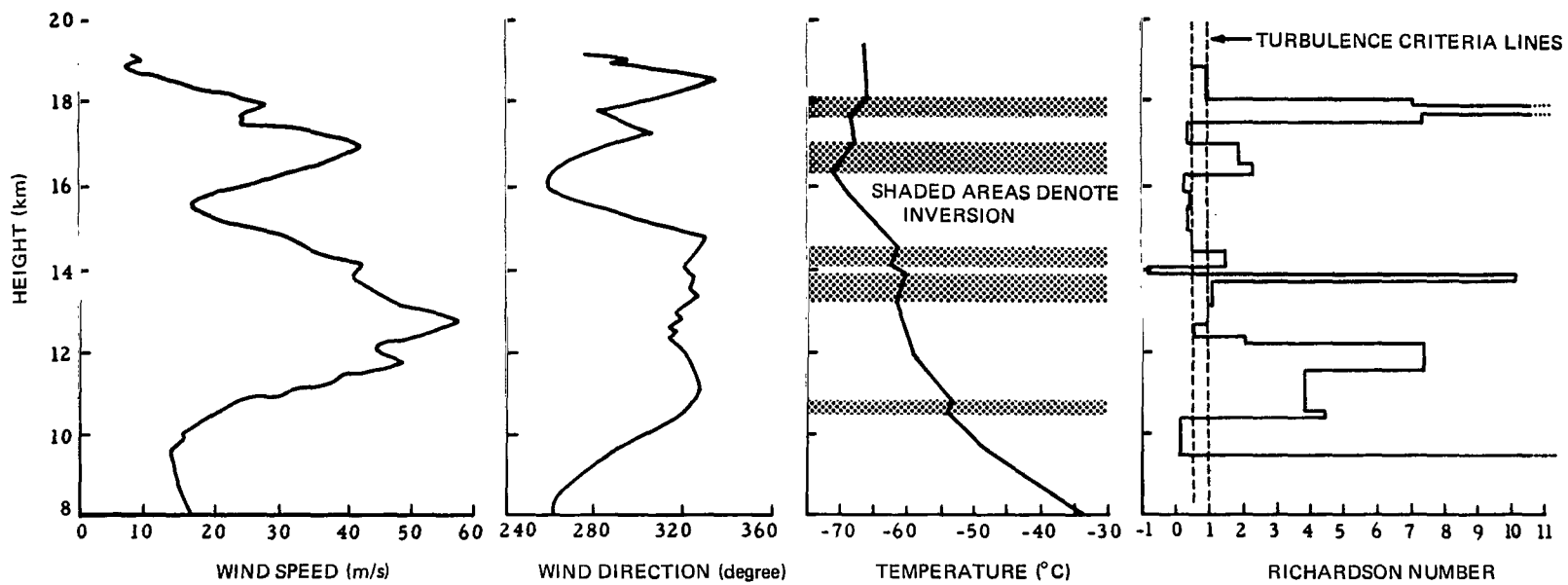
Figure 30. Wind speed, direction, temperature, and Richardson number profiles.

The exact description and interpretation of the profiles of wind, temperature, Ri, and turbulence, and of their development from previous profiles, must await the obtaining of more suitable measurements. The interpretation previously given, based on Figure 30, provides encouragement that the physical principles related to Ri will prove to be valid in this application.

2. Wind Profiles. The present data measure perturbations in a quasi-Eulerian system (quasi because successive balloon soundings do not measure winds in precisely the same location). While this is of no serious consequence in macroscale observations and analysis, it may have some bearing on meso-scale or microscale considerations. Inertial oscillations, however, are defined in the Lagrangian coordinate system. From single-station analysis, therefore, the presence of such oscillations can only be inferred.

Another difficulty is presented by the necessity of removing the "basic" field of flow (the geostrophic wind profile) from the measurements to arrive at the perturbations. This process still involves a certain amount of subjectivity. The data from a single sounding can never give sufficient information to permit the calculation of geostrophic wind to the accuracy desired. Eventually, more accuracy is obtainable by including other wind soundings that differ in time and location and by using three-dimensional temperature field data.

Figure 31 shows, as an example, the wind speed and direction profile for a selected Jimsphere radar measurement. Considering what has been said in describing Figure 29, no phase relationship between peaks in either profile should be expected in an individual sounding because the phase at which the balloon intercepts the successive oscillations remains undetermined.

An inspection of the individual perturbations in successive soundings reveals that the speed and direction of the perturbations vary according to the changing phase of the inertial cycle (Fig. 29). However, such systematic changes are difficult to detect because minor adjustments in "the basic flow profile" to be subtracted from the measured winds may significantly alter the relationship between speed and direction fluctuations. Because of this difficulty, no statistical evaluation of such relationships has been presented. Qualitative evidence in support of such a phase relationship, however, has been observed in the data.
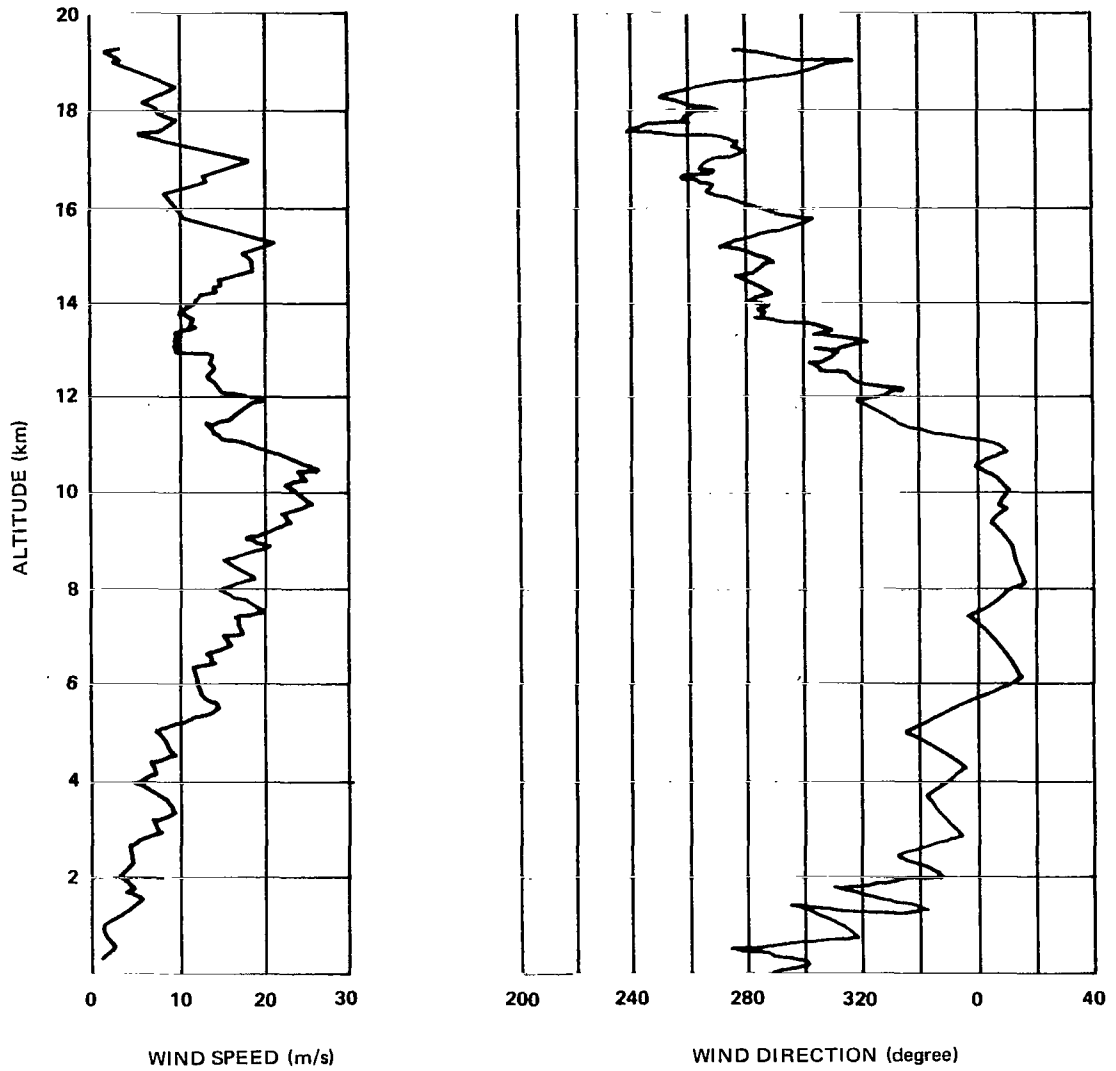
Figure 31. Selected wind speed and direction profiles.

D. Potential Causes of Quasi-Inertial Oscillations

Raethjen (1958) has pointed out that subgeostrophic components of flow may be introduced into the tropopause region by the large convective systems. These systems would transport air masses with relatively small horizontal momentum upwards into an environment with high wind speeds. Such a process could conceivably trigger inertial oscillations downstream from the convective source region.

Mountain ranges also may serve as sources of ageostrophic components on a large scale, by generating low-pressure systems in the upper flow pattern on their lee side, and on a smaller scale by producing mountain waves under suitable atmospheric conditions.

A large number of persistent perturbations in the Jimsphere radar wind profiles are observed above the tropopause level in a thermally stable environment. Strong convective processes in the troposphere may be a potential source for these perturbations. Mountain effects, however, are known to reach to even higher levels in the stratosphere.

Jet stream systems with their associated accelerations and decelerations contain ageostrophic components of flow in deep layers. The thermal structure of the atmosphere also shows a great amount of detail in the vicinity of jet streams (Danielsen, 1959; Reiter, 1963; and Reiter and Mahlman, 1964).

According to Newton (1959), the wavelength, L, of quasi-inertial oscillations is a function of the basic flow, $\bar{v}$, and Coriolis force, f:

$$L = a \; \frac{2\pi}{f} \; \bar{v} \tag{3}$$

(the factor, a, is equal to one for true inertial oscillations and larger than one for oscillations in which the geostrophic field of flow adjusts itself slowly to the perturbations). If in a region of geostrophic vertical wind shear an ageostrophic component of motion is introduced in a deep layer with the same sign and similar magnitude (as might be the case in the vicinity of a jet stream system), the dispersive characteristics of equation (3) would cause a phase shift of inertial oscillations in successive vertical layers of the shearing flow downstream from the source region of the ageostrophic component.

Now postulate that a certain thermal structure, consisting of a succession of more and less stable layers, is originally present in the atmosphere where the inertial oscillations are generated. The vertical wind shears produced by the dispersive properties of equation (3) would lead to exchange processes (fluid flow instability leading to meso- and microscale motion and turbulence) in the less stable regions, and the more stable layers would contain the quasi-inertial oscillations at nearly full magnitude. Wind profiles similar to the ones observed may thus result.

Unfortunately, at this time no details are known concerning the full spatial extent and possible phase changes of the wind perturbations observed by the Jimsphere radar system. The aforementioned reasonings, therefore, must remain speculative.

V. CONCLUSIONS

This research investigation into the mesoscale features of the troposphere and lower stratosphere as revealed by sequential detailed wind profile measurements from the Jimsphere-radar system has resulted in the following conclusions:

1. There are no clear-cut, natural separations between different wave numbers as reflected by the analysis of spectra. Therefore, the division between macroscale, mesoscale, and microscale is arbitrary with respect to the vertical wind profile structure.

2. Mesoscale perturbations in the wind flow may be conserved in time and space up to periods of 12 h or more.

3. The amplitude of speed and direction oscillations appears to be related to major lapse rate discontinuities.

4. The mesostructure of the atmosphere appears to consist of very thin, stable, and relatively large horizontal dimension layers.

5. The quasi-inertial oscillation model with stacked layers provides the best explanation for the observed relatively persistent mesoscale perturbations based on available data.

Future research should be designed to explore the physical nature of the observed mesoscale structural details in the wind profile. This will require the measurement of temperature and pressure with the same detail as provided by the Jimsphere radar system relative to the winds. In addition, simultaneous measurements at several locations (perhaps ~30 km apart) within a nearby geographical area, parallel and normal to mean wind flow, must be designed into the experiment. This would also help establish the degree of coupling that may exist between the principal physical mechanism and other mechanisms in producing the mesostructure features observed.

60

APPENDIX A

ENGINEERING CRITERIA

The various features of the wind profiles and their behavior as a function of time and altitude are of considerable importance in the design and operation of aerospace vehicles. The recent advent of high rate of climb aircraft adds another vehicle to the existing important class of vertically rising rockets and space vehicles. The influence of low wave number of macroscale wind profile features can often be accommodated by wind biasing or trajectory shaping techniques. Conceptually, these techniques can be employed on relatively short time notice prior to actual flight. At least in theory, this could eliminate a considerable protion of the forcing function on the structural and control system due to low wave number wind speed perturbation, if required by a particular vehicle's development limitations and operational requirements. However, the two other categories of wind profile perturbations must be accounted for within the design of the vehicle system, or avoided if possible, during operations by prelaunch monitorship schemes. There is no way to avoid the microscale or turbulent category of the wind profile; therefore, it must be incorporated into the design at a minimum risk level and considered in any prelaunch wind monitorship and flight simulation because it cannot be predicted in a deterministic manner for expected launch inflight winds. This leaves the mesoscale category of wind profile features. It is this category that contains the frequencies of greatest concern to most structural and control system responses (Ryan and King, 1969).

A number of attempts have been made to represent the mesoscale category of the wind profile in a suitable form for use in vehicle engineering studies. Most attempts have resulted in descriptions that could be used for specific applications but, to date, no universal representation has been formulated. Discrete and continuous mesoscale wind structure representations take the form of relatively well-defined, sharp-edged, and repeated sinusoidal characteristics (Daniels, 1973). Sharp edge discrete mesoscale features represented by a quasi-square wave with an amplitude of approximately 9 m s^{-1} is one representation. These are often referred to as embedded jets or singularities in the vertical wind profile and may be observed to develop and persist in the sequential profile measurements. Figures 6 and 7 give excellent examples of this discrete feature in the wind profile. Another form of discrete mesoscale features that has been observed is approximately sinusoidal in nature. An

analysis concentrating on this feature resulted in the data given in Figure A-1. This figure illustrates the approximate number and amplitude of consecutive sinusoidal type features that may occur for aerospace vehicles engineering analysis purposes. It is very important to recognize that oscillations in the vertical wind profile structure having a pure sinusoidal representation are rarely, if ever, observed in nature.

The continuous mesoscale feature representations take the form of spectra. In general, the smaller scale motions associated with vertical detailed wind profiles are characterized by a superposition of discrete gusts and many random wave number components.
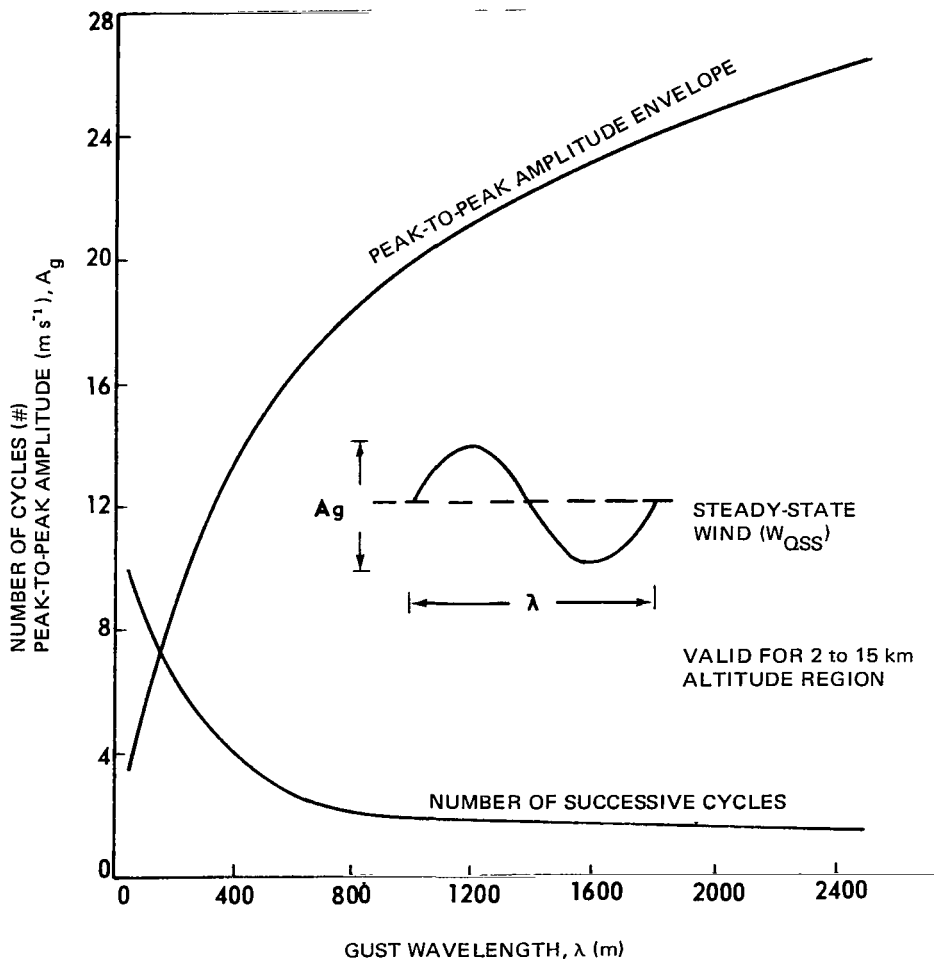

Figure A-1. Best estimate of expected gust amplitude and number of cycles as a function of gust wavelengths.

Spectral methods have been employed to specify the characteristics of this superposition. Spectra have been computed (Fig. A-2 provides one result from the computations) applicable to the 4 to 16 km altitude range. It has been shown (Fichtl, 1972) that the energy of the small scale motions is not vertically homogeneous and may be larger than shown for limited altitude intervals and wave number bands.
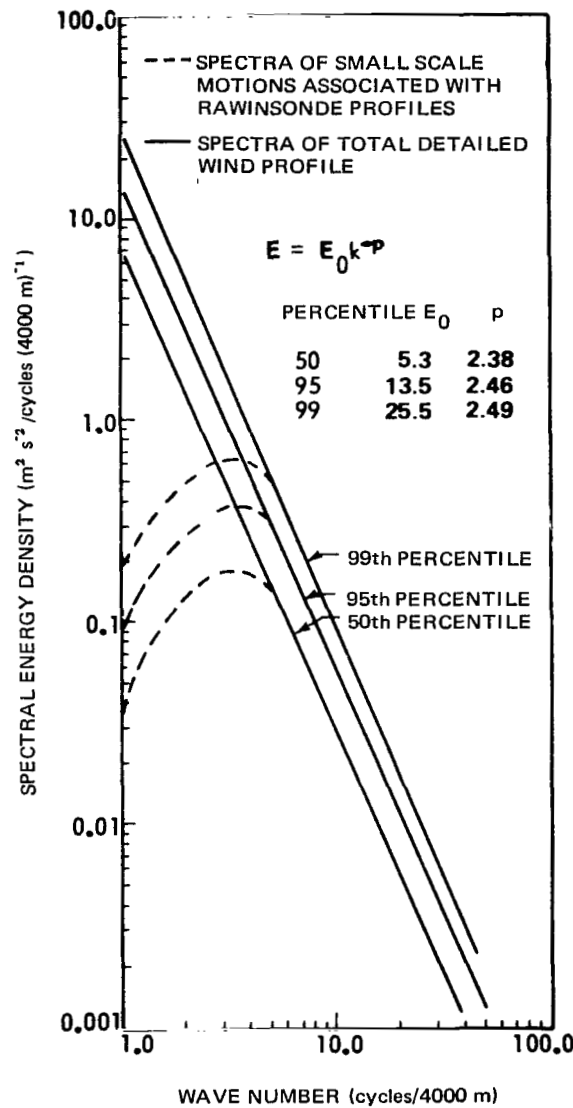

Figure A-2. Spectra of detailed wind profiles.

Use of continuous or power spectrum methods in dynamic response calculations was an important advance over the existing discrete gust method because it took into account the correct variation of energy with wavelength. However, by incorporating the variation of intensity with gradient distance in the discrete method, one can equally include the correct scaling with respect to wavelength. The power spectrum model is concerned with average energy in relatively long patches of wind perturbations and its distribution with wavelength. The discrete gust method is concerned with large local energy concentrations as represented by a localized gradient in the spatial distribution of the wind perturbation. In any particular engineering design situation, the choice of an appropriate wind perturbation model will depend upon the application. In the case of aircraft, for example, the discrete gust method is well suited to treatment of rigid body modes relevant to assessment of control and handling qualities, because these modes need to be well damped. The power spectrum method, however, is appropriate in the case of loads at points in the structure where the dominant response is from a lightly damped structural mode (Jones, 1971).

The mesoscale perturbations shown by the sequential wind profile measurements in Appendix B are of a frequency that affects the performance and response of vertically rising aerospace vehicles. It is important that they be considered in the design and that the vehicle be capable of performing under their influence. It is also important for major launch operations to anticipate the magnitude and characteristics of such oscillations, at least within the range of wavelengths which might trigger response frequencies in the rising vehicle. This would call for highly sophisticated forecasting procedures which, without knowledge of the physical nature of these oscillations, would have to be based entirely on statistical findings. A large data base would be required. Even though some of the observed oscillations persist for several hours, it is not fully understood what causes their appearance or disappearance in any specific sequence of measurements or what physical mechanism maintains them while they are observed. Therefore, based upon the available data analyses and evidence of physical processes responsible for the observed oscillations, only short term forecasts, not to exceed 1 to 3 h, could be issued. A single sounding provides no indication of what possible development the measured mesoscale perturbations might undergo. This is readily evident by observing the behavior of the sequential data sets provided in Appendix B.

APPENDIX B

SEQUENTIAL JIMSPHERE RADAR WIND
PROFILE MEASUREMENTS

Ten sequences of detailed wind speed profiles obtained from measurements made by the Jimsphere radar system were selected to illustrate the various vertical scales of motion. This appendix contains plots of these data (Figs B-1 through B-10). The measurements were made at Cape Kennedy, Florida, and Point Mugu, California. A description of the system is given by Scoggins and Susko (1965) and Scoggins (1967). One is rapidly impressed by the apparent organized wave structure that exists within the troposphere and, especially, the lower stratosphere. It is evident that there must exist a principal mechanism with, perhaps, numerous secondary mechanisms that provide perturbations and thereby produce the rather complex behavior in the wind flow. The analysis of these and similar data sets, plus other sequential measurements reported in the main body of the text, provided the basis for this study. See Johnson and Alexander (1976) for plots of other data sets.
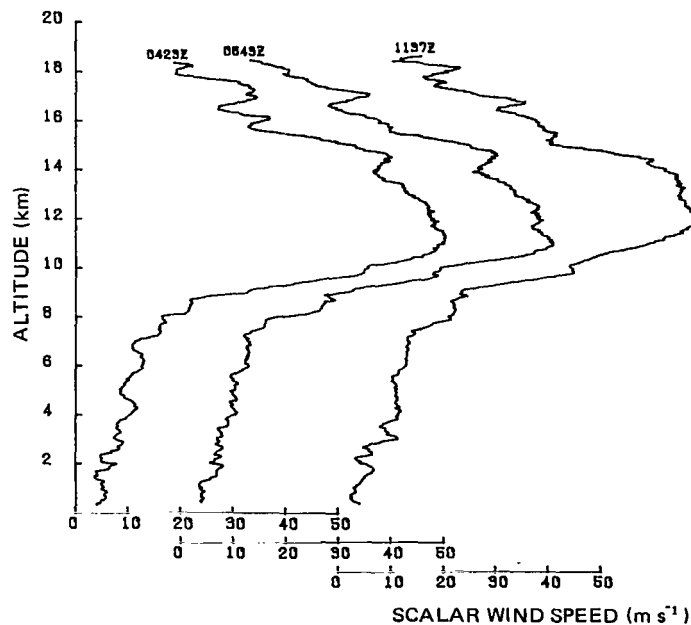

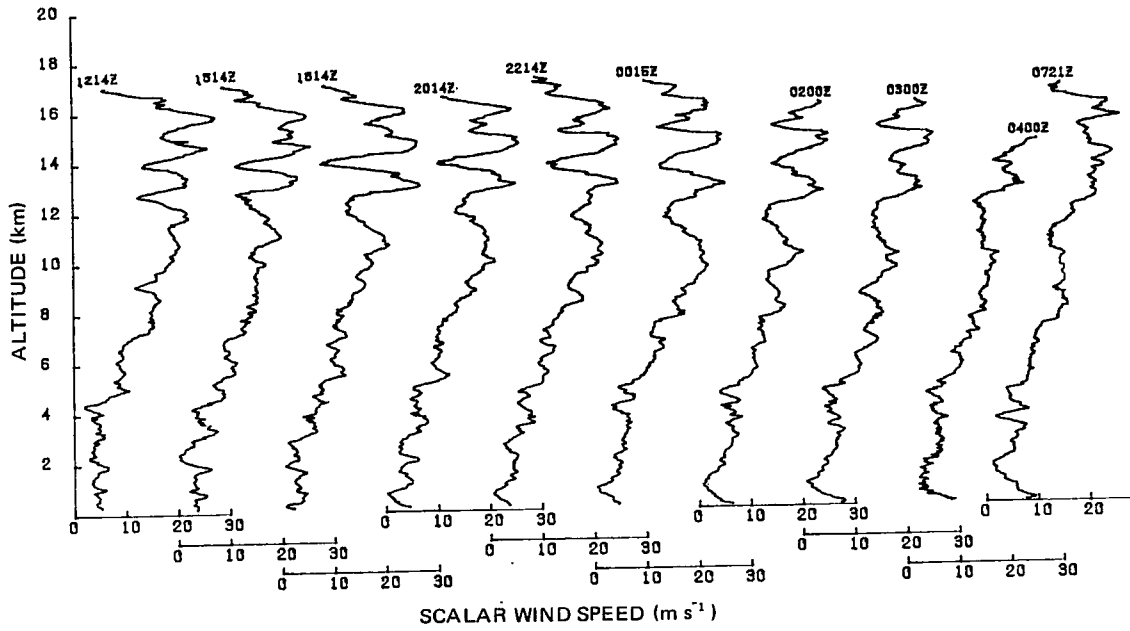Figure B-1. Cape Kennedy Jimsphere wind profile data, February 7, 1966.

Figure B-2. Cape Kennedy Jimsphere wind profile data,
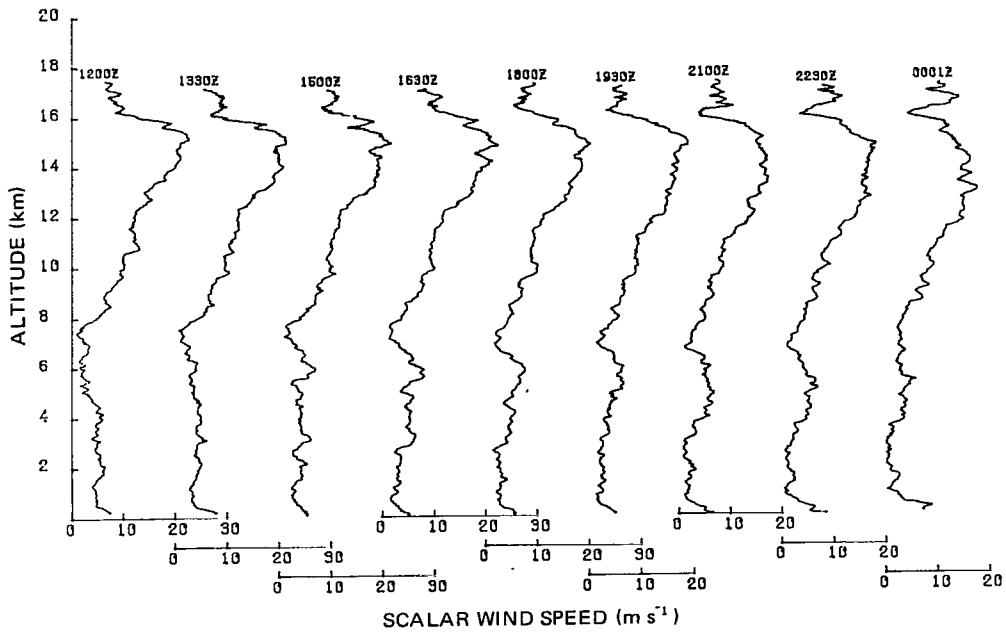April 16-17, 1967.

Figure B-3. Cape Kennedy Jimsphere wind profile data,
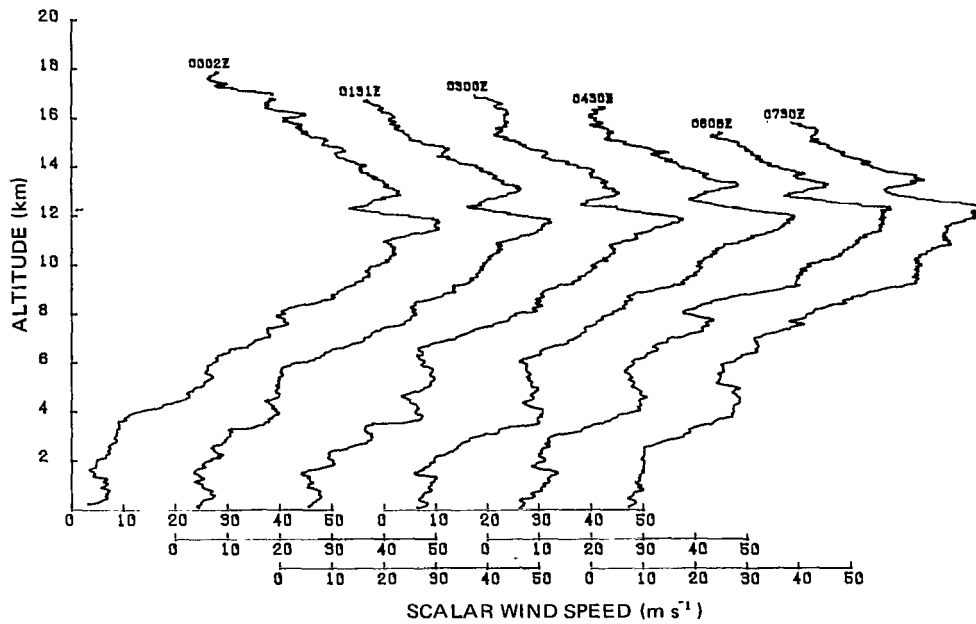August 19-20, 1968.

Figure B-4.   Cape Kennedy Jimsphere wind profile data,
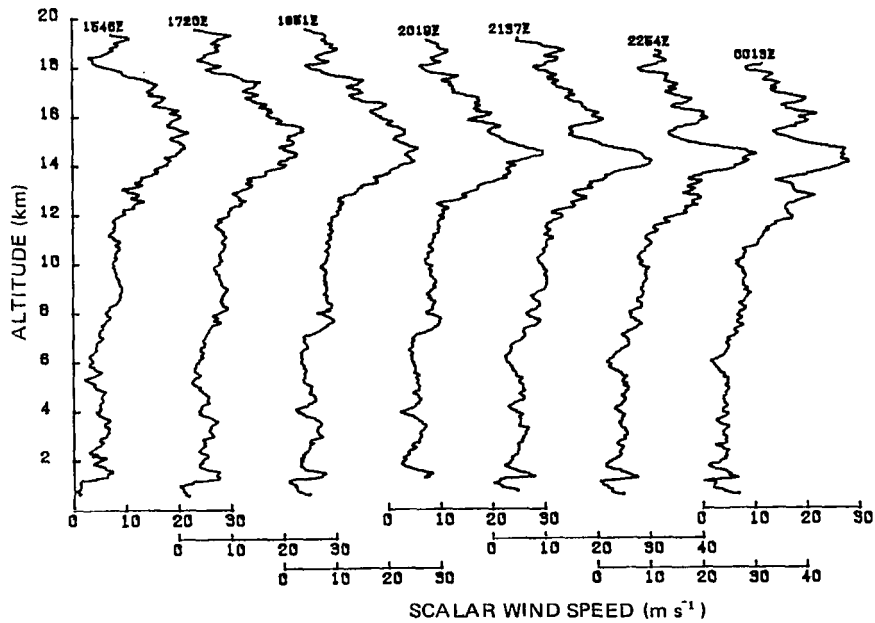February 11, 1969.

Figure B-5.   Point Mugu Jimsphere wind profile data,
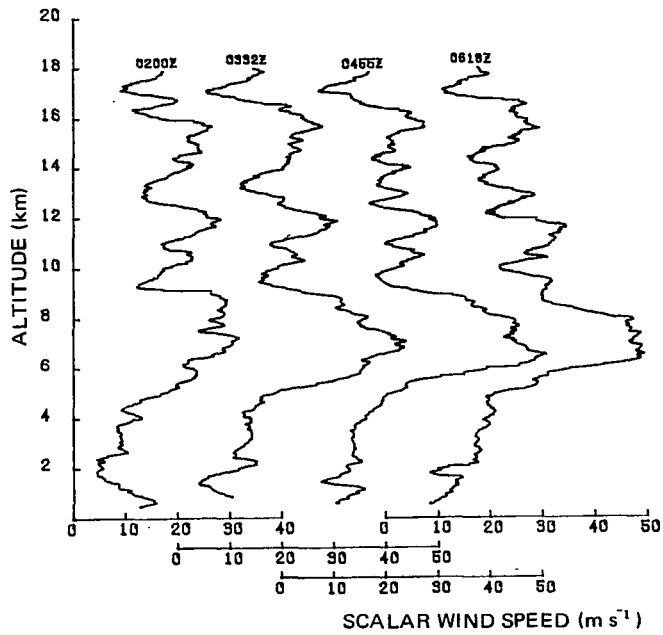May 12-13, 1969.

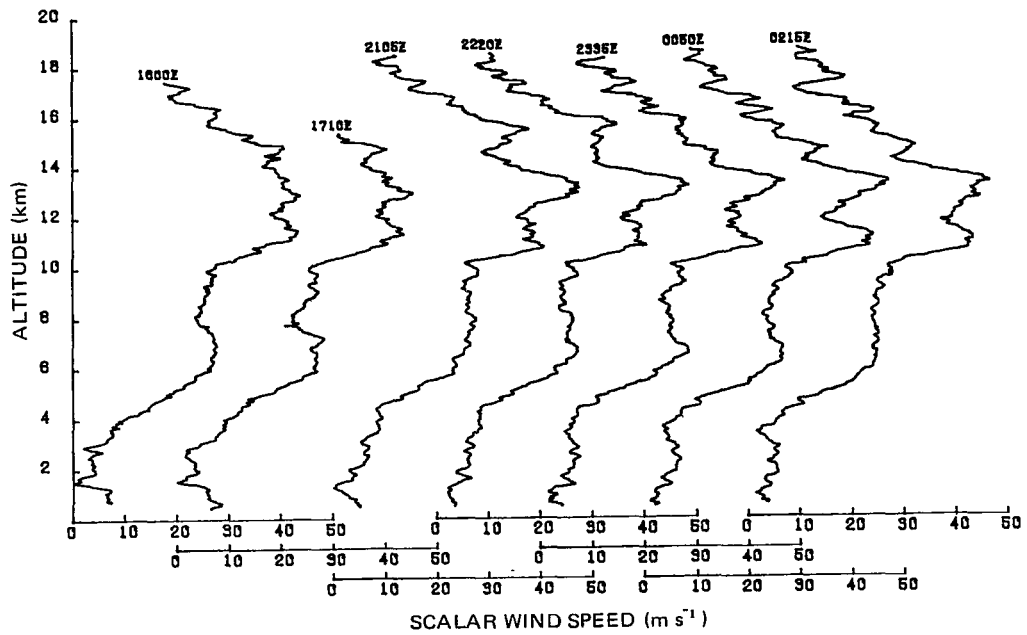Figure B-6. Point Mugu Jimsphere wind profile data, December 22, 1965.

Figure B-7. Point Mugu Jimsphere wind profile data, March 2-3 1965.
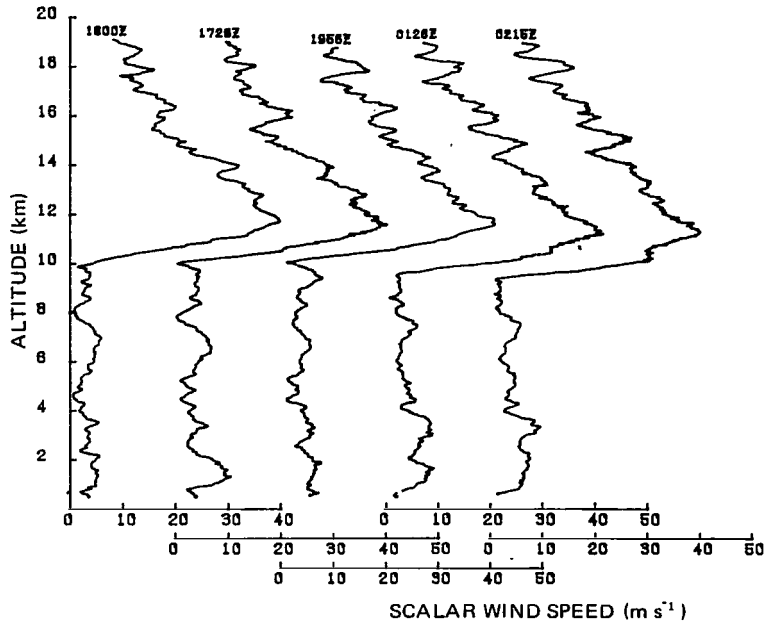
Figure B-8. Point Mugu Jimsphere wind profile data,
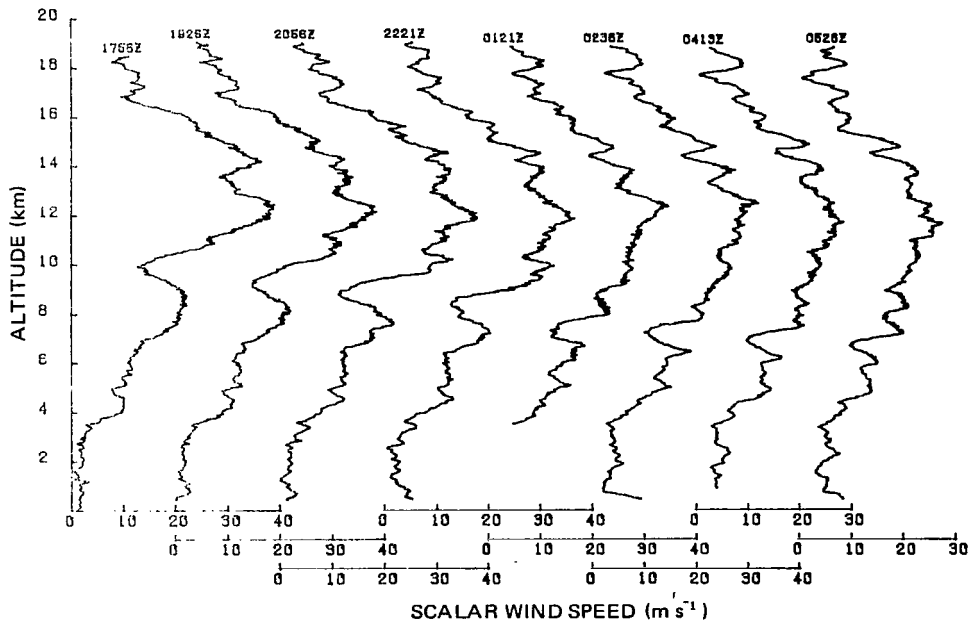February 18-19, 1965.

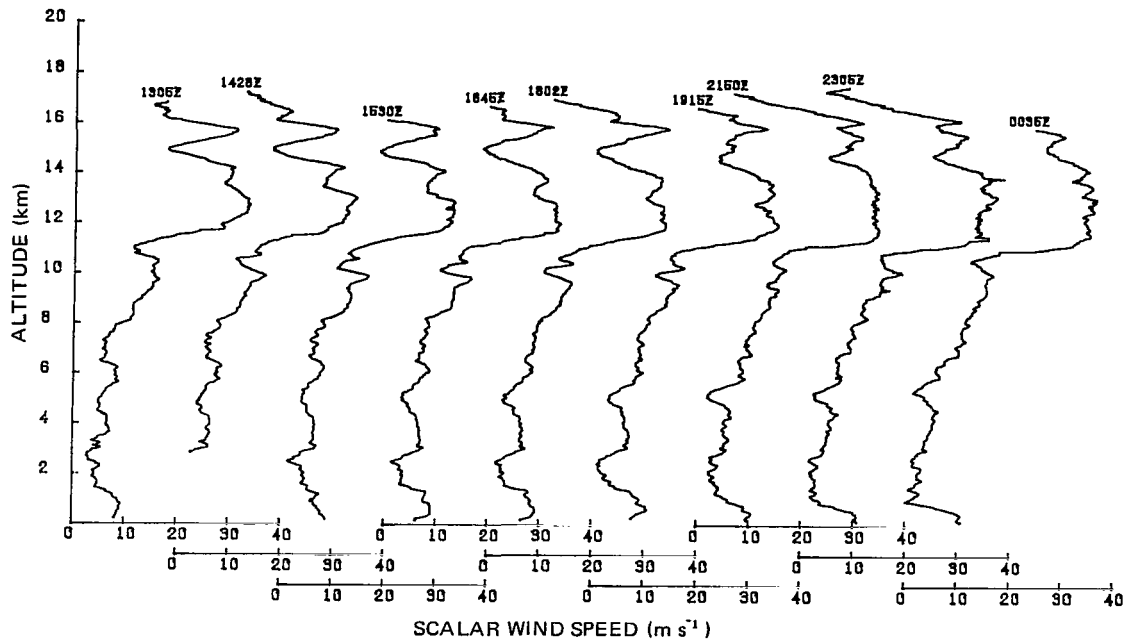Fibure B-9. Point Mugu Jimsphere wind profile data,
January 18-19, 1965.

Figure B-10. Cape Kennedy Jimsphere wind profile data,
February 10-11, 1965.

REFERENCES

Avsec, Dusan (1939): Thermoconvective Eddies in Air Application to Meteorology. Sci. and Tech. Publ. of Air Ministry Works, Inst. of Fluid Mech., Fac. of Sci., Paris, no. 155. [Translated from French by C. Ronne, Woods Hole Ocean. Inst., Woods Hole, Massachusetts].

Barbé, G. D. (1958): Donnees sur le Vent en Altitude. J. Sci. Meteor., vol. 10, pp. 47-67.

Bekofske, Deith Laverne (1972): The Interaction of Internal Gravity Waves and Atmospheric Winds with Shear. Ph.D. Dissertation, The University of Michigan.

Benard, H. (1936): P. Idrac and the Theory of Clouds in Bands. La Météorologie, no. 3, May-June, 1936.

Bingham, C., M. D. Godfrey, and J. W. Tukey (1967): Modern Techniques of Power Spectral Estimation. IEEE Trans. on Audio and Electroacoustics, vol. AU-15, no. 2, pp. 56-66.

Blackman, R. B. and J. W. Tukey (1958): The Measurement of Power Spectra. Dover Publ., Inc.

Brunt, D. (1939): Physical and Dynamical Meteorology. Cambridge University Press.

Clem, LeRoy H. (1959): Clear-Air Turbulence at High Levels. Proc. Toronto Meteor. Conf., 1953, Roy. Meteor. Soc.

Conover, John H. (1960): Cirrus Patterns and Related Air Motions Near the Jet Stream as Derived by Photography. J. Meteor., vol. 17, pp. 532-546.

Cooley, J. W. and J. W. Tukey (1965): An Algorithm for the Machine Calculation of Complex Fourier Series. Mathematics of Computation, vol. 19, no. 90, pp. 297-301.

Curry, M. J. and R. C. Murty (1974): Thunderstorm-Generated Gravity Waves. J. Atmos. Sci., vol. 31, pp. 1402-1408.

REFERENCES (Continued)

Daniels, Glenn E. (1973): Terrestrial Environment (Climatic) Criteria Guidelines for Use in Aerospace Vehicle Development. 1973 Rev., NASA TM X-64757.

Danielsen, Edwin F. (1959): The Laminar Structure of the Atmosphere and Its Relation to the Concept of a Tropopause. Archiv fur Meteorologie, Geophysik and Bioklimatologie, Series A: Meteorologie and Geophysik, Band 11, vol. 3, pp. 293-332.

Danielsen, Edwin F. (1964): Confirmation of Mass Transport as a Form of Stratospheric-Tropospheric Exchange. Program of Amer. Meteor. Soc., 44th Annual Meeting, January 29-31, Los Angeles, California.

DeMandel, R. E. and James R. Scoggins (1967): Mesoscale Wave Motions as Revealed by Improved Wind Profile Measurements. J. Appl. Meteor., vol. 6, pp. 617-620.

DeMandel, R. E. and S. J. Krivo (1971): Radar/Balloon Measurements of Vertical Air Motions Between the Surface and 15 km. J. Appl. Meteor., vol. 10, pp. 313-319.

Duffy, Dean G. (1974): Resonant Interactions of Internal-Gravity and Rossby Waves. J. Atmos. Sci., vol. 31, pp. 1218-1231.

Dutton, John A. (1976): The Ceaseless Wind. McGraw-Hill.

Eckstrom, Clinton V. (1965): Theoretical Study and Engineering Development of Jimsphere Wind Sensor. Final Report (NASA Contract NAS8-1158), Marshall Space Flight Center, Huntsville, Alabama.

Endlick, R. M., R. C. Singleton, K. A. Drexhage, and R. L. Mancuso (1969): Studies of Vertical Wind Profiles at Cape Kennedy, Florida. NASA CR-61263.

Fichtl, G. H., D. W. Camp, and W. W. Vaughan (1968): Detailed Wind and Temperature Profiles. Clear Air Turbulence and Its Detection (Yih-Ho Pao and Arnold Goldberg, eds.), Plenum Publishing Company, pp. 308-333.

REFERENCES (Continued)

Fichtl, George H. (1972): Small-Scale Wind Shear Definition for Aerospace Vehicle Design. J. Spacecraft and Rockets, vol. 9, pp. 79-83.

Fredler, Franz and Hans A. Panofsky (1970): Atmospheric Scales and Spectral Gaps. Bull. Amer. Meteor. Soc., vol. 51, pp. 1114-1119.

Goldie, A. H. R. (1925): Waves at an Approximately Horizontal Surface of Discontinuity in the Atmosphere. Quart. J. Roy. Meteor. Soc., vol. 51, pp. 239-246.

Gossard, E. E., J. H. Richter, and D. Atlas (1970): Internal Waves in the Atmosphere from High Resolution Radar Measurements. J. Geophys. Res., vol. 75, pp. 3523-3536.

Gossard, Earl E. and William H. Hooke (1975): Waves in the Atmosphere. Elsevier Scientific Publishing Co.

Hess, Seymour L. (1959): Introduction to Theoretical Meteorology. Holt, Rinehart, and Winston.

Hines, C. O. (1960): Internal Atmospheric Gravity Waves at Ionospheric Heights. Canadian J. Phys., vol. 38, pp. 1441-1481.

Hines, C. O. and C. A. Reddy (1967): On the Propagation of Atmospheric Gravity Waves through Regions of Wind Shear. J. Geophys. Res., vol. 72, pp. 1015-1033.

Hinze, J. O. (1975): Turbulence. McGraw-Hill.

Hooke, William H. and Kenneth R. Hardy (1975): Further Study of the Atmospheric Gravity Waves Over the Eastern Seaboard on March 8, 1969. J. Appl. Meteor., vol. 14, pp. 31-38.

Johnson, Dale and Margaret Alexander (1976): Sequential Jimsphere Wind Profile Data Sets. Report No. NASA/MSFC-ES41, Marshall Space Flight Center, Huntsville, Alabama.

Jones, J. C. (1971): A Unified Discrete Gust and Power Spectrum Treatment of Atmospheric Turbulence. International Conference on Atmospheric Turbulence, London, England, May 1971. [AIAA Reprint No. A71-29790].

Jones, Walter L. and David D. Houghton (1972): The Self-Destructing Internal Gravity Wave. J. Atmos. Sci., vol, 29, pp. 844-849.

Jordan, A. Raymond (1972): Atmospheric Gravity Waves from Winds and Storms. J. Atmos. Sci., vol. 29, pp. 445-456.

Kao, S. K. and W. Neiburger (1959): Oscillations and Trajectories of Air Particles in Some Pressure Systems. J. Geophys. Res., vol. 64, pp. 1283-1291.

Kao, S. K. and H. D. Woods (1964): Energy Spectra of Mesoscale Turbulence Along and Across the Jet Stream. J. Atmos. Sci., vol. 21, pp. 513-519.

Kuettner, Joachin (1959): The Band Structure of the Atmosphere. Tellus, vol. 11, pp. 267-294.

Lloyd, K. H., C. H. Low, and R. A. Vincent (1972): Features of Atmospheric High Shear Region. Radio Sci., vol. 21, pp. 653-661.

Lumley, J. L. (1964): The Spectrum of Nearly Inertial Turbulence in a Stably Stratified Fluid. J. Atmos. Sci., vol. 21, pp. 99-102.

Lumley, J. L. and H. A. Panofsky (1964): The Structure of Atmospheric Turbulence. John Wiley and Sons.

Manning, James C., Robert M. Henry, and Robert W. Miller (1966): Wind Velocity Profiles Measured by the Smoke-Trail Method at the Eastern Test Range, 1962. NASA TN D-3289.

Mee, Rhomas R. (1964): An Investigation of Convective Cells Over the Ocean. Final Report to Applied Oceanography Group (Contract SD 75543-0), Scripps Institution of Oceanography, San Diego, California.

REFERENCES (Continued)

Miller, Robert W., Robert M. Henry, and Mickey G. Rowe (1965): Wind Velocity Profiles Measured by the Smoke Trail Method at Wallops Island, Virginia, 1959 to 1962. NASA TN D-2937.

Murrow, Harold N. and Robert M. Henry (1965): Self-Induced Balloon Motions. J. Appl. Meteor., vol. 4, pp. 131-138.

Neiburger, M. and J. K. Angell (1956): Meteorological Applications of Constant Pressure Balloon Trajectories. J. Meteor., vol. 13, pp. 166-194.

Newell, R. E., J. R. Mahoney, and R. W. Lenhard, Jr. (1966): A Pilot Study of Small-Scale Wind Variations in the Stratosphere and Mesosphere. Quart. J. Roy. Meteor. Soc., vol. 92, pp. 41-53.

Newton, Chester W. (1959): Axial Velocity Streaks on the Jet Stream: Ageostropic "Inertial" Oscillations. J. Meteor., vol. 16, pp. 638-645.

Pack, D. (1962): Air Trajectories and Turbulence Statistics from Weather Radar Using Tetroons and Radar Transponders. Monthly Weather Rev., vol. 90, pp. 491-506.

Pinus, N. Z. (1963): Statistical Characteristics of the Horizontal Components of the Wind Velocity at Heights of 6-12 km. Bull. Acad. Sci., USSR, Geophys. Ser., pp. 105-107.

Pinus, N. S., E. R. Reiter, G. N. Shur, and N. Vinnichenko (1967): Power Spectra of Turbulence in Free Atmosphere. Tellus, vol. 19, pp. 206-213.

Raethjen, P. (1958): Traegheitsellipse und Jet Stream. Geophysica Helsinki, vol. 6, pp. 439-453.

Reed, R. J., K. Azim, and E. V. von Gohren (1964): Observational Evidence of Mesoscale Wave Motion in the Stratosphere and Mesosphere. Program of Amer. Meteor. Soc., 44th Annual Meeting, January 29-31, Los Angeles, California.

REFERENCES (Continued)

Reiter, E. R. (1958): The Layer of Maximum Wind. J. Meteor., vol. 15, pp. 27-43.

Reiter, E. R. (1963): A Case Study of Radioactive Fallout. J. Appl. Meteor., vol. 2, pp. 691-705.

Reiter, E. R. and J. D. Mahlman (1964): Heavy Radioactive Fallout Over the Southern United States, November 1962, from Transport Processes in the Atmosphere Leading to Radioactive Fallout. Dept. of Atmospheric Science Tech. Paper No. 58, Colorado State University.

Reiter, Elmar R. (1969): Structure of Vertical Wind Profiles. Radio Sci., vol. 4, pp. 1113-1136.

Rogers, R. R. and H. G. Camitz (1965): Project Building — An Investigation of Aerodynamically Induced Balloon Motions. Final Report (NASA Contract NAS8-11140), Marshall Space Flight Center, Huntsville, Alabama.

Ryan, Robert S. and Alberta W. King (1969): The Influential Aspects of Atmospheric Disturbances on Space Vehicle Design Using Statistical Approaches for Analysis. NASA TN D-4963.

Sawyer, J. S. (1961): Quasi-Periods Wind Variations with Height in the Lower Stratosphere. Quart. J. Roy. Meteor. Soc., vol. 87, pp. 24-33.

Schaefer, V. J. (1957): The Relationship of Jet Streams to Forest Fires. As Referred to by Conover (1960).

Schlichting, Hermann (1960): Boundary Layer Theory. McGraw-Hill.

Scoggins, James R. (1963): An Evaluation of Detail Wind Data as Measured by the FPS-16 Radar/Jimsphere Balloon Technique. NASA TN D-1572.

Scoggins, James R. and Michael Susko (1965): FPS-16 Radar/Jimsphere Wind Data Measured at the Eastern Test Range. NASA TM X-53290.

REFERENCES (Continued)

Scoggins, James R. (1965): Spherical Balloon Wind Sensor Behavior. J. Appl. Meteor., vol. 4, pp. 139-145.

Scoggins, James R. (1967): Sphere Behavior and the Measurement of Wind Profiles. NASA TN D-3994.

Scorer, R. S. (1949): Theory of Waves in the Lee of Mountains. Quart. J. Roy. Meteor. Soc., vol. 75, pp. 41-56.

Scorer, R. S. (1951): On the Stability of Stably Stratified Shearing Layers. Quart. J. Roy. Meteor. Soc., vol. 77, pp. 76-84.

Smith, T. B. and M. A. Wolf (1963): Vertical Diffusion from an Elevated Line Source Over a Variety of Terrains. Final Report to Dugway Proving Ground (Contract DA 42-007-CML-545) (AD 418 599, Part A), Meteorology Research, Inc., Dugway, Utah.

Susko, Michael and William W. Vaughan (1968): Accuracy of Wind Data Obtained by Tracking a Jimsphere Wind Sensor Simultaneously with Two FPS-16 Radars. NASA TM X-53572.

Tatarski, V. I. (1961): Wave Propagation in a Turbulent Medium. McGraw-Hill.

Taylor, G. I. (1917): Observations and Speculations on the Nature of Turbulent Motions. [Reprinted from from reports and memoranda of the Advisory Committee for Aeronautics no. 345 (1917) in the scientific papers of Sir Geoffrey Ingram Taylor, vol. II]. Cambridge University Press, 1960, pp. 69-78.

Todd, J. (1962): Survey of Numerical Analysis. McGraw-Hill.

Vinnichenko. N. K. and T. A. Dutton (1969): Empirical Studies of Atmospheric Structure and Spectra in the Free Atmosphere. Radio Sci., vol. 4, pp. 1120-1132.

REFERENCES (Concluded)

Vinnichenko, N. K., N. Z. Pinus, S. M. Shmeter, and G. N. Shur (1973): Turbulence in the Free Atmosphere. Translated from Russian by Consultants Bureau, New York.

Weinstein, A. L. and E. R. Reiter (1965): Mesoscale Structure of 11-20 km Winds. NASA CR-61080.

Whitten, R. C. and C. A. Riejel (1973): Internal Gravity Waves in an Atmosphere with Wind Shear: Validity of the WHB Approximation at Critical Layers in the Presence of Buoyance Forces. J. Atmos. Sci., vol. 30, pp. 313-316.

Woodcock, A. H. (1942): Soaring Over the Open Sea. Scientific Monthly, September, pp. 226-232.

"The aeronautical and space activities of the United States shall be conducted so as to contribute . . . to the expansion of human knowledge of phenomena in the atmosphere and space. The Administration shall provide for the widest practicable and appropriate dissemination of information concerning its activities and the results thereof."
—NATIONAL AERONAUTICS AND SPACE ACT OF 1958

NASA SCIENTIFIC AND TECHNICAL PUBLICATIONS

TECHNICAL REPORTS: Scientific and technical information considered important, complete, and a lasting contribution to existing knowledge.

TECHNICAL NOTES: Information less broad in scope but nevertheless of importance as a contribution to existing knowledge.

TECHNICAL MEMORANDUMS: Information receiving limited distribution because of preliminary data, security classification, or other reasons. Also includes conference proceedings with either limited or unlimited distribution.

CONTRACTOR REPORTS: Scientific and technical information generated under a NASA contract or grant and considered an important contribution to existing knowledge.

TECHNICAL TRANSLATIONS: Information published in a foreign language considered to merit NASA distribution in English.

SPECIAL PUBLICATIONS: Information derived from or of value to NASA activities. Publications include final reports of major projects, monographs, data compilations, handbooks, sourcebooks, and special bibliographies.

TECHNOLOGY UTILIZATION PUBLICATIONS: Information on technology used by NASA that may be of particular interest in commercial and other non-aerospace applications. Publications include Tech Briefs, Technology Utilization Reports and Technology Surveys.

Details on the availability of these publications may be obtained from:

SCIENTIFIC AND TECHNICAL INFORMATION OFFICE

NATIONAL AERONAUTICS AND SPACE ADMINISTRATION

Washington, D.C. 20546